REPORT DOCUMENTATION PAGE

Form Approved
OMB No. 0704-0188

1. REPORT DATE *(DD-MM-YYYY)*	2. REPORT TYPE	3. DATES COVERED *(From - To)*
31-03-2011	Book Chapter	

4. TITLE AND SUBTITLE

Chapter 18 - Propulsion Systems

5a. CONTRACT NUMBER

5b. GRANT NUMBER

5c. PROGRAM ELEMENT NUMBER

6. AUTHOR(S)
Ivett A. Leyva, Marcus Young, William A. Hargus Jr., Richard Van Allen, Charles M. Zakrzwski

5d. PROJECT NUMBER

5f. WORK UNIT NUMBER
23070725

7. PERFORMING ORGANIZATION NAME(S) AND ADDRESS(ES)

Air Force Research Laboratory (AFMC)
AFRL/RZSA
10 E. Saturn Blvd.
Edwards AFB CA 93524-7680

8. PERFORMING ORGANIZATION REPORT NUMBER

AFRL-RZ-ED-BK-2011-057

9. SPONSORING / MONITORING AGENCY NAME(S) AND ADDRESS(ES)

Air Force Research Laboratory (AFMC)
AFRL/RZS
5 Pollux Drive
Edwards AFB CA 93524-7048

10. SPONSOR/MONITOR'S ACRONYM(S)

11. SPONSOR/MONITOR'S NUMBER(S)
AFRL-RZ-ED-BK-2011-057

12. DISTRIBUTION / AVAILABILITY STATEMENT

Approved for public release; distribution unlimited (PA #10985).

13. SUPPLEMENTARY NOTES
For publication in textbook: "Space Mission and Analysis Design"

14. ABSTRACT

This chapter starts with a review of the basic rocket performance parameters, the rocket equation and staging. Different classes of chemical rockets used for space propulsion are then examined. The System Design Elements section guides the reader on how to size common components for a conventional chemical propulsion system. Electric propulsion and other potential new systems are presented next. This chapter concludes with two examples of preliminary designs for a propulsion system.

15. SUBJECT TERMS

16. SECURITY CLASSIFICATION OF:			17. LIMITATION OF ABSTRACT	18. NUMBER OF PAGES	19a. NAME OF RESPONSIBLE PERSON
a. REPORT	b. ABSTRACT	c. THIS PAGE			Dr. Ivett A. Leyva
Unclassified	**Unclassified**	**Unclassified**	SAR	71	19b. TELEPHONE NUMBER *(include area code)* N/A

18. Propulsion Systems

Ivett A. Leyva, ***Air Force Research Lab, Edwards AFB, CA***

This chapter starts with a review of the basic rocket performance parameters, the rocket equation and staging. Different classes of chemical rockets used for space propulsion are then examined. The System Design Elements section guides the reader on how to size common components for a conventional chemical propulsion system. Electric propulsion and other potential new systems are presented next. This chapter concludes with two examples of preliminary designs for a propulsion system. Commonly used references in the field of rocket propulsion are: Sutton and Blibarz [2010], Turner [2009], Hill and Peterson [1992], Jahn [1968], Micci and Ketsdever [2000], Brown [2002], Brown [1996] and Humble [1995].

The first task of a propulsion system is to propel a spacecraft from the Earth's surface to an initial or parking orbit using one of the launch vehicles discussed in Chap. 26. Depending on the desired final orbit, an onboard propulsion system or an upper stage might be needed to provide the final boost. Chapters 9 and 10 offer a detailed description of orbits. As the spacecraft performs its mission, when its orbit needs to be closely controlled, an onboard propulsion system also accomplishes orbit maintenance (Chap. 9), de-orbit (Chap. 30) and reentry operations. Beside translational movements, rotational movements are needed as well to keep a satellite pointing in the right direction. This is achieved through what is called attitude control (Sec. 19.1). An onboard propulsion system can either perform attitude control maneuvers or it can be used to unload momentum from onboard equipment, such as reaction wheels.

Propulsion systems distinguish themselves by their energy source and how they produce thrust. With the exception of a few cases, the propulsion systems discussed in this chapter produce thrust by accelerating and ejecting a fluid through a converging-diverging nozzle. The oldest and most common type of propulsion system is a *chemical rocket* in which propellants combust producing high temperature products that are then expanded through a nozzle. The historic rockets that propelled the

Apollo missions, those most commonly used on launch vehicles and missiles, and even the rockets that the Chinese used nearly 1000 years ago all fall under this category. Other types of propulsion systems are nuclear and solar. In *nuclear rockets,* propellants are heated through nuclear fission of certain materials like uranium. In *solar propulsion,* energy from the sun is collected and used to produce thrust. Some designs use solar energy directly to heat a propellant which can then be expanded through a nozzle to produce thrust. Alternatively, in solar sails, discussed in Sec. 18.7, the pressure from solar photon bombardment pushes against a sail to produce low levels of thrust. In *electric propulsion*, discussed in detail in Sec. 18.6, solar or nuclear energy is converted to electrical energy to either heat and then accelerate a propellant, or directly accelerate a propellant through electric and magnetic body forces. Finally, missions with minimal propulsive needs can use a *cold gas thruster*, where a non-reacting high-pressure gas is accelerated through a nozzle. Because of their similarities with chemical propulsion systems, cold gas thrusters are presented in Sec. 18.3.

In designing a propulsion system, the first step is to determine the objectives of the mission. Is it an interplanetary mission? Is the spacecraft to be placed in LEO or GEO? How long will the spacecraft be functional? What are the top level constraints on cost, schedule, and what is the risk allowed to try a new propulsion technology? Are there any political angles to the mission that need to be taken into consideration? For example, are international partners available? Does the nature of the payload bias the choice for a propulsion system? For example, having very sensitive instruments might put a constraint on what kind of exhaust you can have from a propulsion system. The orbit of the spacecraft needs to be determined at this stage as well.

Designing a propulsion system is by nature a multidisciplinary effort. Once the top level objectives for the mission are set, the lower level requirements for the propulsion system can be addressed. For a detailed discussion of this process see Humble [1995]. Table 18-1 lists a series of considerations for determining the propulsion system for a given mission. In step 1 list all the functions the propulsion system will have to fulfill for the duration of the mission, i.e. from orbit insertion to de-orbit. In steps 2 and 3 get quantitative details on performance requirements like ΔV, thrust, and total impulse needed from the propulsion system. In Step 4 list the available propulsion systems to meet the above requirements. Don't try to select a system at this point, just list the available options. In step 5, list all the quantifiable figures of merit for the propulsion system, such as thrust, I_{sp}, propellant mass, propellant mass fraction and volume. Qualitative factors also have a big play on ranking different propulsion systems. For example, a system which has been successfully used before and can meet the requirements could directly provide a design solution. Also, if the people in the team have experience with a particular rocket type, this might also play into the decision of which one to choose. In step 6, reach a consensus with the team on what factors matter the most. Once the weight factors are determined for each quantitative requirement, you can proceed to rank the different options and choose a baseline in step 7. Document your decisions and how you arrived to them. More often than not, as the design matures the requirements change, making you reconsider the choices for propulsion systems. Keep flexibility in mind and be prepared for your design to change over time.

Table 18-1. Propulsion Subsystem Selection and Sizing Process

Step	References
1. Determine all the functions the propulsion system must accomplish such as orbit insertion orbit maintenance attitude control controlled de-orbit or re-entry **Establish the life expectancy of the mission.**	Table 18- 2
2. Determine the required ΔV and thrust for orbit insertion and orbit maintenance	Table 18- 2, Sec. 18.1, Sec. 14.5.2
3. Determine the required total impulse, thrust level for control authority, and duty cycles for attitude control	Table 18- 2
4. List propulsion system options Chemical (solid, liquid [monopropellant, bipropellant], hybrid, cold gas) vs. electric propulsion or other. Single or separate propulsion systems for orbit maintenance and attitude control (if needed)	Secs. 18.3, 18.6
5. Estimate key parameters for each option (some will be quantitative as below but others might be qualitative, consider both)	
I_{sp}	Sec. 18.1
Thrust	Sec. 18.1
Total mass (including propellant mass)	Propellant budget mass Subsystem mass table
Power requirements	Power Table
System volume including tankage, thrust chamber, feedlines, valves, etc.	
"ilities" such as reliability (if system has been tried before, what has been the success rate), manufacturability, storability, scalability, vulnerability	
Cost, schedule, acceptable risk for program	
Toxicity of propellants and character of plume (especially if it can interact with critical instruments or parts of the spacecraft and generate inadvertent torque)	Sec. 18.4

6. Conduct Trade Studies	
Choose a baseline propulsion system	
Document trade results and the reasons for those results. Iterate the process as necessary	

18.1 Basic rocket equations

The thrust of rocket engines is most often measured in stationary thrust stands. Load cells are typically used to measure the force that the engine imparts on the supporting structure. Note that we can measure thrust without much knowledge of how it is produced. Following the analysis of Hill and Peterson [1992], we use a control volume (CV) to understand the relationship between thrust and flow conditions (Fig. 18-1). In this case, the CV encloses the rocket and cuts through the structure holding it in place. By inspection, we can see that the rocket does not produce forces in the y-direction, so we are only interested in the forces in the x-direction. Following the analysis presented in Hill and Peterson [1992], Newton's second law in the x-direction results in

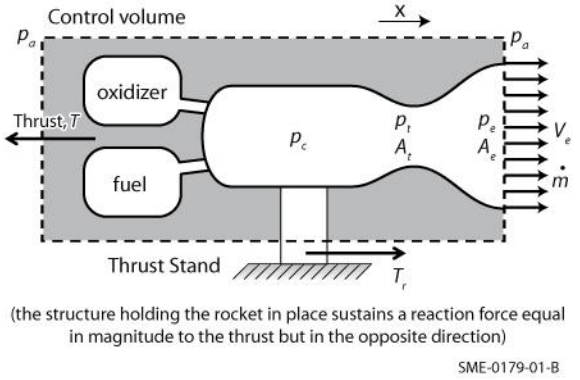

Figure 18- 1. Control Volume around a rocket on a static test stand.

$$\sum \vec{F}_x = \frac{d}{dt}\int_{CV} \rho \vec{v_x} dVo + \int_{CS} \rho \vec{v_x} \vec{v_x} \bullet \vec{dA} \qquad (18\text{-}1)$$

Where ρ denotes density and v_x is the velocity in the x-direction. The first term on the right hand side is the time rate of change of the integral of the momentum per unit volume (dVo) over the control volume (CV). The second term is the flux of momentum through the control surface (CS). The left side of the equation represents the sum of forces, F_x, acting ***on*** the control volume in the x-direction. These are the pressure forces and the force from the support on the control volume (T_r), which has the same magnitude as the thrust but opposite direction (Newton's 3rd law). Let's assume T_r is in the positive x-direction since the support has to exert a force to the right to counteract the rocket thrust.

Evaluating the terms on the left and right hand sides of Eq. 18-1, and for the case of steady operation, we have,

$$T_r + p_a A_e - p_e A_e = \dot{m} V_e \qquad (18\text{-}2)$$

$$T_r = \dot{m} V_e + A_e (p_e - p_a) \qquad (T_r \text{ acts in the positive x-direction}) \qquad (18\text{-}3)$$

where A_e is the exit area of the rocket nozzle, $\dot{m}$ is the mass flow rate being expelled through the nozzle (mass the rocket is losing per unit time), p_e and p_a are the nozzle exit plane and ambient pressures respectively, and V_e is the nozzle exhaust velocity. Since $\dot{m}\, V_e$ is positive and dominates over the second term for practical operating conditions, the reaction force T_r will be in the positive x-direction.

The thrust, T, and the reaction force T_r have the same magnitude but act in opposite directions as required by Newton's 3rd law. The resulting expression for thrust is then:

$$T = \dot{m} V_e + A_e (p_e - p_a) \qquad (T \text{ acts in the negative x-direction}) \qquad (18\text{-}4)$$

Examining Eq. 18-4 we see from the first term that thrust depends on how much mass you eject from the engine and the velocity it attains as it leaves the nozzle. The second term represents a mismatch between the nozzle exit plane and the ambient pressures. As the rocket travels through the atmosphere and p_a changes, this force changes and it can add to or subtract from the thrust. For upper stage engines and in-space propulsion systems p_a is close to or equal to zero.

To increase thrust, we could increase V_e by using a larger nozzle exit area (A_e) while keeping the same chamber temperature and pressure, chemical composition, and throat area. However, this would result in a lower p_e, which could have adverse effects if p_e drops below p_a. This is why large area ratios (A_e /A_{throat}) are preferred in upper stage engines where the rocket is fired at very low values of atmospheric pressure or at vacuum. However, we must make a trade-off between the extra thrust produced and the additional weight of a larger nozzle.

For a fixed area ratio, we can increase V_e and thrust by increasing the chamber pressure or temperature, which can be accomplished by changing the fuel/oxidizer mixture ratio or the propellants used. Increasing the chamber pressure would require thicker (heavier) walls. Increasing the flame temperature would require more cooling (which degrades performance) or more expensive materials. Finally, we can augment thrust by increasing $\dot{m}$. This could, however, imply a shorter burn time for a given amount of propellants or more propellants to carry which would require larger and heavier tanks.

If we divide the thrust (Eq. 18-4) by the mass flow rate exhausting from the nozzle, we obtain the *equivalent or effective exhaust velocity,* which is a measure of how efficiently the engine produces thrust. Some authors denote this velocity as *c*.

$$V_{eq} = \frac{T}{\dot{m}} = V_e + \left(\frac{p_e - p_a}{\dot{m}}\right) A_e \qquad (18\text{-}5)$$

Note that when p_e equals p_a, V_e equals V_{eq}.

A relatively easy way to measure the performance of a rocket in a static stand is by measuring *c**, (pronounced c star) which is the *characteristic exhaust velocity*,

$$c^* = \frac{p_c A_t}{\dot{m}} \tag{18-6}$$

where p_c is the chamber pressure and A_t is the throat area. This is a measure of the efficiency of the combustion. Note that it is independent of the nozzle design. Values for *c** range from 1333 m/s for hydrazine (N_2H_4), 1640 m/s for hypergolic systems of N_2O_4 and MMH (monomethylhydrazine), and up to 2360 m/s for liquid oxygen (LOX)-liquid hydrogen (LH_2) systems. Experimental results, though, are usually given in terms of *c** efficiency against the theoretical values computed from thermochemistry. Efficiency values (c^*_{exper}/c^*_{theor}) are usually in the range of 96-98%.

Rocket Equation and Specific Impulse. To derive the famous rocket equation, let's start with a free body diagram (Fig. 18-2) showing the forces acting on a rocket as it flies through the atmosphere. T is the thrust produced by the rocket (assumed to act along the longitudinal axis of the vehicle); V is the velocity of the rocket; D is the drag force, which is opposite to the direction of flight; L is the lift force, which is perpendicular to the direction of flight; Mg is the weight of the rocket; V_e is the velocity of the exhaust from the rocket nozzle, and $\dot{m}$ is the mass ejected through the nozzle per unit time. Please note that due to gravity and the aerodynamic forces (D and L), the direction of flight (γ) does not coincide with the direction of thrust (θ). Also note that to keep accelerating upward, the thrust produced by the rocket has to overcome both the drag and the weight of the vehicle. In practice, at launch we want the thrust to the weight ratio, T/Mg, to be on the order of 1.3 to have acceptable accelerations.

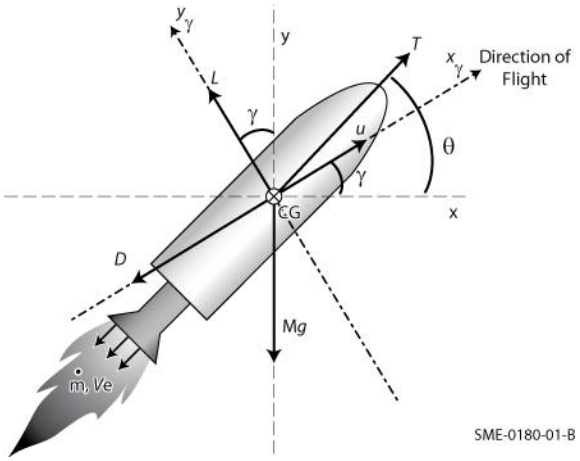

Figure 18- 2. Forces acting on a rocket as it flies.

For convenience of analysis, let's apply Newton's 2nd law in the direction of flight (γ),

$$\sum F_{\gamma} = M\frac{dV}{dt} = T\cos(\theta-\gamma) - D - Mg\sin\gamma \tag{18-7}$$

As time passes, the terms in the above equation change (e.g., the mass of the rocket (M) decreases as a function of time, winds affect the aerodynamic forces), and the direction of flight can change as well. If the direction of flight changes, it means our x_γ-y_γ coordinate system has rotated with respect to the fixed x-y coordinate system. Remember, by definition we are choosing x_γ to be aligned with the direction of flight. Thus, accounting for the possible rotation of the axes, the acceleration in the direction perpendicular to flight is given by,

$$\sum F_{\perp\gamma} = MV\frac{d\gamma}{dt} = T\sin(\theta-\gamma) + L - Mg\cos\gamma \tag{18-8}$$

To calculate the velocity attained by a rocket after a certain time, we integrate Eq. 18-7, from an initial time t_o to a final time t_f.

$$\frac{dV}{dt} = \frac{T}{M} - \frac{T}{M}\left[1-\cos(\theta-\gamma)\right] - \frac{D}{M} - g\sin\gamma \tag{18-9}$$

$$\int_{Vo}^{Vf} dV = \int_{t_o}^{t_f}\frac{T}{M}dt - \int_{t_o}^{t_f}\frac{T}{M}\left[1-\cos(\theta-\gamma)\right]dt - \int_{t_o}^{t_f}\frac{D}{M}dt - \int_{t_o}^{t_f} g\sin\gamma dt \tag{18-10}$$

$$\Delta V = \Delta V_{prop} - \Delta V_{steering} - \Delta V_{drag} - \Delta V_{gravity} \tag{18-11}$$

Equation 18-11 shows how the drag, weight, and the fact that the thrust is not in the direction of flight, subtract from the thrust force produced by the rocket. The losses due to gravity and drag are about 1500-2000 m/s for LEO.

If drag and gravity can be ignored, which also means that θ=γ, and we substitute the expression for V_{eq} from Eq. 18-5 into Eq. 18-10 realizing that $\dot{m} = -dM/dt$, we get,

$$\Delta V = \int_{t_o}^{t_f}\frac{T}{M}dt = V_{eq}\int_{t_o}^{t_f}\frac{\dot{m}}{M}dt = -V_{eq}\int_{M_o}^{M_f}\frac{dM}{M} \tag{18-12}$$

$$\Delta V = -V_{eq}\ln\left(\frac{M_f}{M_o}\right) = V_{eq}\ln\left(\frac{M_o}{M_f}\right) = V_{eq}\ln\left(\frac{M_o}{M_o - M_p}\right) \tag{18-13}$$

This is the *ideal rocket equation* first introduced by Russian schoolteacher Konstantin Tsiolkovsky (1857-1935) in 1903, where M_o is the initial mass, M_f is the mass after the burnout time, and M_p is the propellant mass defined as,

$M_p = M_o - M_f$ (18-14)

The *mass ratio* has been defined by different authors as either M_f/M_o or M_o/M_f. We will be using the rocket equation later in our examples section (18.8).

For solid rocket motors in particular, the *total impulse*, I, is an important performance parameter defined as the integral of thrust, T, over the burn time, t,

$$I = \int_0^t T(t)dt \tag{18-15}$$

This quantity is the energy released by a propulsion system. If the thrust is constant over the burn time, the total impulse is simply the product of the thrust times the burn time.

The *specific impulse*, is usually defined as the total impulse normalized by the weight of the propellants. For constant thrust force and uniform propellant mass flow rate the specific impulse reduces to,

$$I_{sp} = \frac{T}{\dot{m} g_o} = \frac{V_{eq}}{g_o} \tag{18-16}$$

where T is the thrust, $\dot{m}$ is the mass flow rate, and g_0 is the gravitational constant at the Earth's surface, 9.80665 m/s^2, which gives a value of I_{sp} expressed in seconds in SI units. The expression in terms of V_{eq} comes from using Eq. 18-5. The use of the constant g_0 is in fact arbitrary, depending on whether the total impulse was normalized by the mass or the weight of the propellants. It can be thought of as a conversion factor and does not change where the gravitational acceleration is different. If omitted, I_{sp} is expressed in m/s and becomes the effective exhaust velocity of Eq. 18-5. Whether one uses g_0 or not to compute I_{sp} has been matter of confusion in the rocket community so keep good track of units when dealing with I_{sp} values.

We can see that I_{sp} is a measure of how efficiently we produce thrust. In a sense, it is similar to the specific fuel consumption for a gas turbine or miles per gallon for a car. Analyzing the expression for I_{sp} (Eq. 18-16) we can see that higher values of I_{sp} reduce the propellant rate needed to achieve a given amount of thrust. For launch propulsion systems, thrust is more important than I_{sp} because you must have enough force to get off the ground and through the atmosphere. For upper stage engines and in-space propulsion, I_{sp} is more important because the weight has been significantly reduced and you want to minimize the propellant you carry.

**********Move to Side Bar all text in green **********

A simplified relationship between specific impulse, I_{sp}, chamber temperature, T_c, and exhaust species molecular weight, MW, is given by,

$$I_{sp} = \sqrt{\frac{R_u T_c}{MW}\frac{2k}{k-1}\left[1-\left(\frac{p_e}{p_c}\right)^{\frac{k-1}{k}}\right]} + \frac{p_e - p_a}{p_c} c^* \varepsilon \qquad (18\text{-}17)$$

where k is the ratio of the specific heats c_p/c_v (assumed constant for reactants and products). Usually this ratio is denoted by γ but to avoid confusion with γ from Eqs. 18-7 to 10, it is denoted k in this formula. R_u is the universal gas constant (8.314472 J/mol K), p_e is the nozzle exhaust pressure, p_C is the combustion chamber pressure, p_a is the ambient pressure, ε is the nozzle area expansion ratio; namely the nozzle exit area divided by the throat area, A_e/A_t, and c^* is the characteristic exhaust velocity defined in Eq. (18-6). From this expression we see why it is preferred to have exhaust gases with low molecular weight such as the water vapor produced when H_2 and O_2 are used as propellants. Also, we see why the higher the combustion temperature the higher the specific impulse.

Substituting Eq. (18-16) into the ideal rocket equation (18-13) we obtain an expression in terms of I_{sp},

$$\Delta V = I_{sp} g_o \ln\left(\frac{M_o}{M_f}\right) \qquad (18\text{-}18)$$

where we can see that ΔV is linear with I_{sp} so any improvements on the specific impulse have a big effect on ΔV. Because the rocket equation is so widely used the following alternate forms, solving for the propellant mass, can be very useful for preliminary design calculations as we will see in the examples at the end of this Chapter.

$$M_p = M_f\left(e^{\Delta V/V_e} - 1\right) = M_f\left(e^{\Delta V/I_{sp}g_o} - 1\right) \qquad (18\text{-}19)$$

$$M_p = M_o\left(1 - e^{-\Delta V/V_e}\right) = M_o\left(1 - e^{-\Delta V/I_{sp}g_o}\right) \qquad (18\text{-}20)$$

Figure 18-3 shows the effect on ΔV from systems with different I_{sp} values as a function of the ratio of the propellant mass to the final mass after the propellant has been burned out, M_p/M_f. For launch vehicles this ratio might approach 5-10 but for in-space propulsion it ranges from 0.2 to 1, showing how hard it is to achieve the required ΔV to at least reach LEO. In ascending order, the values of I_{sp} selected are representative of cold gas thrusters, monopropellant, solid and high performing liquid rockets, as we will see later. We can see that the higher the I_{sp} the higher the ΔV achieved for a given mass ratio. Also, for a given I_{sp}, you want to maximize the mass ratio to achieve the largest ΔV values.

As a common practice, the requirements for a propulsion system are listed in terms of ΔV, thrust, total impulse, number of pulses and duration of the pulses from the rocket. Table 18- 2 shows typical requirements for different functions a propulsion system has to execute. Table 18-3 serves as an overview of how different propulsions systems, to be studied in the rest of this chapter, can be used for different applications along with typical ranges for their I_{sp}.

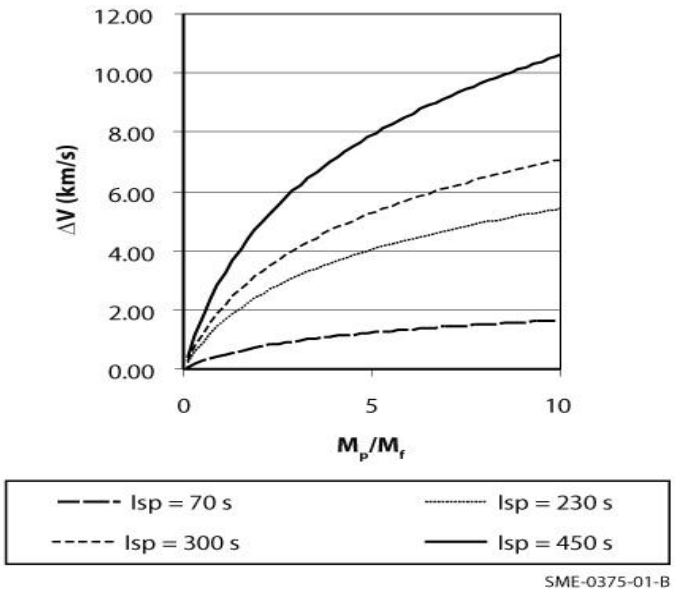

Live Calc

Figure 18- 3. ΔV as a function of M_p/M_f and I_{sp}.

Table 18- 2. Typical functions and requirements for upper stages and in-space propulsion.

Propulsion Function	**Typical ΔV and Other Requirements**
Orbit Transfer to GEO (orbit insertion)	
Perigee Burn	2400 m/s
Apogee Burn	1500 (low inclination) to 1800 m/s (high inclination)
Initial Spin up	1-60 rpm
LEO to higher orbit raising ΔV	60-1500 m/s
Drag makeup ΔV	60-500 m/s
Controlled reentry ΔV	120-150 m/s
Acceleration to escape velocity from LEO parking orbit	3600-4000 m/s into a heliocentric orbit
Orbit Maintenance	
Despin	60 to 0 rpm
Spin control	± 1 to ±5 rpm
Orbit correction ΔV	15 to 75 m/s per year
East-West stationkeeping ΔV	3 to 6 m/s per year
North-South stationkeeping ΔV	45 to 55 m/s per year
Survivability or evasive maneuvers (highly variable) ΔV	150 to 4600 m/s
Attitude Control	3-10% of total propellant mass
Acquisition of Sun, Earth, Star	low total impulse, typically <5000 N-s, 1K to 10K

	pulses, 0.01 to 5.0 s pulse width
On-orbit normal mode control with 3-axis stabilization, limit cycle	100K to 200K pulses, minimum impulse bit of 0.01 N-s, 0.01 to 0.25 s pulse width
Precession control (spinners only)	low total impulse, typically <7000 N-s, 1K to 10K pulses, 0.02 to 0.2 s pulse width
Momentum management (wheel unloading)	5 to 10 pulse trains every few days, 0.02 to 0.10 s pulse width
3-axis control during ΔV	on-off pulsing, 10K to 100K pulses, 0.05 to 0.20 s pulse width

Table 18-3. Overview of common applications for different propulsion systems.

Propulsion System	Orbit Insertion		Orbit Maintenance and Maneuvering	Attitude Control	Typical Range of I_{sp} (s)
	Perigee	Apogee			
Cold Gas			**X**	**X**	**45-73**
Solid	**X**	**X**			**290-300**
Liquid					
Monopropellant			**X**	**X**	**200-235**
Bipropellant	**X**	**X**	**X**	**X**	**274-466**
Electric		**X**	**X**	**X**	**500-3000**

18.2 Staging

There is no launch vehicle today that can place a payload to at least LEO with a single stage. Therefore, the question is not whether your vehicle will have stages but rather how many. The answer usually lies between 2 and 6 depending on the particular mission [Sutton and Blibarz, 2010]. Having more than 1 stage is advantageous because you dispose of the mass of the expended stage (e.g., rocket engines, tanks, remaining propellant) so you don't have to waste energy to propel empty tanks or unusable engines throughout the mission. Also, if you have more than 1 stage, your propellant tanks can be smaller since they carry less mass. With each added stage though, you add complexity to the vehicle design such as more inter-stage structure, joints, separation mechanisms, and separate engines and

tanks. Therefore, it is recommended that you use as few stages as needed to achieve the mission objectives.

To analyze the performance of multiple stages, we use the same equations derived before. For each stage, the ΔV is calculated as before

$$\Delta V_i = V_{eq_i} \ln(\frac{M_{oi}}{M_{fi}}) \tag{18-21}$$

Where i refers to the stage in question, V_{eqi} is the effective exhaust velocity of stage i, M_{oi} is the total mass of the vehicle before the stage i ignites (including all subsequent stages and payload), M_{fi} is the final mass of the vehicle after stage i is expended but before it separates. The total gain in velocity for all the stages is the sum of the individual gains:

$$\Delta V_t = V_{eq_1} \ln(\frac{M_{o1}}{M_{f1}}) + V_{eq_2} \ln(\frac{M_{o2}}{M_{f2}}) + V_{eq_3} \ln(\frac{M_{o3}}{M_{f3}}) + \ldots \tag{18-22}$$

It can be shown [Sutton and Blibarz, 2010] that for a 2-stage vehicle, with similar effective exhaust velocities and I_{sp}, a greater payload mass is achieved when the two stages have the same mass ratio M_{oi}/M_{fi} rather than the same mass. In that case, the stages are said to be similar and it follows that ΔV is the same for each stage. This result extends to more than 2 stages. However, as you go to more stages, the gains on payload mass become smaller and smaller: about 8-10% for a third stage and 3-5% for a fourth stage [Sutton and Blibarz, 2010]. In practice, the performance (e.g., I_{sp}, thrust, M_{prop}/M_o) of the propulsion systems for the different stages is different so the partition of ΔV needs to be optimized to get the largest payload fraction, defined as

$$\lambda = M_{payload}/M_o \tag{18-23}$$

Hill and Peterson [1992] show an analytical method to optimize the ΔV distribution. Ideally, once you have assigned ΔV's to the different stages, you start sizing the vehicle from the top down, sizing first the final stage. For a given ΔV needed, the maximum payload fraction is achieved if 1) stages with higher I_{sp} are above those with lower I_{sp}; 2) the higher the I_{sp} of a stage the more ΔV it should contribute [Wertz and Larson, 2003]; 3) a small increase in I_{sp} is more effective in upper stages than in lower stages, that is why the usual choice of LOX/H_2 systems for upper stages [Sutton and Blibarz, 2010].

18.3 Chemical Propulsion Systems

18.3.1 Cold Gas Thrusters. As mentioned in the introduction, cold gas thrusters don't rely on combustion to produce thrust, but there are enough similarities with chemical propulsion systems to cover them here. Like in chemical rockets, the thrust from cold gas thrusters originates from expanding high pressure gases through a converging-diverging nozzle and the thrust equation (18-4) applies. However, the chamber pressure is only as high as the reservoir tank, and there is no temperature rise due to chemical reactions. Cold gas thrusters are used in cases when the thrust and I_{sp} requirements are

low and a small impulse bit is important. Generally they are used for total impulse up to about 22,000 N-s [Sutton and Blibarz, 2010]. Their main use is for attitude control and small ΔV applications. The I_{sp} of the commonly used gases like He, N_2, and Freon-14 are 165 s, 73 s, and 45 s respectively [Micci and Ketsdever, 2000]. Hydrogen could also be used (I_{sp}~ 272 s) but both H_2 and He have the worst risk of leaks because of the small size of the molecules. The main advantage of cold gas systems is their simplicity. In a typical cold gas thruster system there are only valves, filters, regulators and relief valves connecting the storage high pressure tank to the thruster (Fig. 18-8). Historic examples of systems using cold gas propulsion systems include 1) the Viking Orbiter using N_2 thrusters (I_{sp} = 68 s) on its reaction control system [Brown, 1996; Holmberg, 1980], 2) the Landsat 3 using Freon-14 thrusters for attitude control [Brown, 1996; Landsat 1978] and 3) the manned maneuvering unit used by shuttle astronauts for extra vehicular activities in 1984, which was powered by N_2 cold gas thrusters [Bergonz, 1982]. Table 18-4 shows some examples of available cold gas thrusters.

18.3.2. Liquid Rocket Engines (LREs). Liquid rocket engines (LREs) can be used throughout a mission. They can be used as first and upper stage engines to propel a payload into its initial orbit. LREs can also be used for orbit insertion, maintenance, maneuvering, and attitude control. Some launch vehicles, like the Saturn 5, utilized LREs solely for the first stage. Others like Ariane 5, Atlas 5, Delta 4, and the Space Shuttle (to retire circa 2011), utilize a combination of liquid and solid rockets for liftoff (see Chap. 26 for more details on launch vehicles). For attitude control especially, liquid rockets are preferred because of their capability for multiple restarts [Brown, 1996]

LREs can be classified in several ways. One way is to classify LREs depending on whether turbopumps are used to pressurize the propellants before they enter the combustion chamber or whether high pressure tanks are used instead. The simplicity of the pressure-fed configuration needs to be traded with the additional weight of the heavier, thick-walled tanks needed to hold the propellants at high pressure. LREs are also classified according to their work cycle; that is how they ultimately produce thrust. Common types of cycles are gas generators, expanders, and oxygen-rich staged combustion. See Sutton and Blibarz [2010] for a detailed explanation on these cycles. Finally, LREs are also classified according to the type of propellants they use. Thus, there are monopropellant and bipropellant engines.

Table 18-4. Example of cold gas thrusters. References: [1] Courtesy of AMPAC In-Space Propulsion, and Schappell [2005], [2] Bzibziak [2000], [3] Bzibziak [2010]. * Includes feedback sensor, Isolation valve and nozzle heater

ENGINE	Manufacturer	Status	Engine Mass (kg)	Length (m)	Propellants	Nominal Thrust (N)	Specific Impulse (s)	Operating Pressure (kPa)
SVT01 Solenoid Valve thruster[1]	AMPCA	Flown on SNAP-1, DMC Alsat, UK,	0.051	0.021	Butane, GN2, Xe, CF4	0.01-0.05	70 GN2, 45 CF4	150 to 1000

		etc						
Proportional microNewton Thruster[1]	AMPAC	Qualification Test Demonstrated on Engineering Model	0.281*	0.10*	GHe, GN2, Dry air	Up to 0.001	70 GN2	100 to 500
Solenoid Actuated 58E142A Thruster[2, 3]	Moog	Flown on SIRTF/SPITZER	Up to 0.016	~0.032	GN2	0.12 at 690 kPa	>57	340 to 2070
Solenoid Actuated 58-118 Thruster [2, 3]	Moog	Flown on SAFER (Shuttle EVA)	0.022	~0.0254	GN2	3.5	>70 (71.5-73)	1482

Monopropellants. In a monopropellant system, like the name suggests, there is one propellant which decomposes exothermically as it passes through a catalytic bed. This results in heated high pressure gases which are expanded through a converging diverging nozzle to produce thrust. One advantage of a monopropellant system is that it avoids the mixing step of a two-propellant system which could lead to combustion roughness or even instabilities. A typical system consists of a pressurization system, a propellant tank, a propellant valve, a catalyst bed (including a heater for the catalyst material) and a converging-diverging nozzle. Table 18-5 shows some examples of monopropellant thrusters, some of which are shown in Fig. 18-4. In general, monopropellant systems have an I_{sp} range from 165-244 s and they are used for ΔV requirements of 1000 m/s or less [Micci and Ketsdever, 2000]. The propellants of choice today are hydrazine, N_2H_4, and hydrazine blends. Hydrazine first decomposes into hydrogen and ammonia (T_{flame} ~ 1700 K) when it comes into contact with the catalyst bed. Subsequently, the ammonia decomposes into nitrogen and hydrogen in an endothermic reaction lowering the flame temperature to about 1394 K. Therefore, one aspect of the design of hydrazine monopropellant systems is how to limit further dissociation of ammonia to achieve the best I_{sp} [Brown, 1996]. The main advantages of hydrazine are its relatively high I_{sp} [230 s], system simplicity, long term storability, clean exhaust, stability, restart capability, and low flame temperature [Brown, 1996]. The main disadvantages are its lower I_{sp} compared to bipropellants, its toxicity, and high freezing point at 274K [Thompson, 2001]. Therefore, research is being conducted to find alternative monopropellants which are safer to handle and have lower freezing points, such as amine azides [Thompson, 2001]. Today, granular alumina coated with iridium is commonly used for catalyst beds. The size of the catalyst bed is in part driven by the time the propellant needs to be in contact with the catalyst. One of the main concerns with the operation of monopropellant systems is the degradation of the catalyst bed over the mission life.

Degradation is a function of the total amount of propellant used, mass flow rate or operating pressure, number and size of thermal cycles, and number of pulses.[1] Catalyst bed heaters are almost always used to preheat the bed prior to operation in order to increase bed life and to also decrease the ignition delay. Monopropellant systems used for attitude control need to be able to restart multiple times. How quickly thrust can be generated is also important. Other factors to consider when designing a monopropellant system are how fast the valve responds, how fast the catalyst heats up so that it can promote decomposition of the propellant, and how fast the pressure rises [Brown, 1996].

Table 18-5. Representative Monopropellant Systems. References: [1] Sweetman [2006], [2] Courtesy of AMPAC In-Space Propulsion, [3] Northrop [2010a], [4] McRight [2005], [5] Swink [1999], [6] Frei [2001], [7] Morrisey [1992] and Dawnson [2007], [8] Astrium [2010b]. (v)= vacuum

[1] As a note, because of the smaller mass flow rates, microsatellites (10-100 kg) will likely incur less degradation [Ketsdever, 2006].

ENGINE	Manufacturer	Status	Engine Mass (kg)	Length (m)	Propellants	Nominal Thrust (N)	Specific Impulse (s)	Total Impulse (N-s)
Liq AOCS thrusters[1]	SEP	D5a, spot, geos, exosat, geos, exosat, ERS, Helios, Envisat	0.320/0.355	0.108/0.145	hydrazine	3.5-16.5 (v) at max p	230/232 (v)	
MONARC-5[2]	AMPAC In-Space Propulsion	Flight qualified	0.49	0.203	Hydrazine	4.5	233	4.60E+05
MONARC-90[2]	AMPAC In-Space Propulsion	Flight qualified	1	0.3	Hydrazine	90	235	3.50E+06
MONARC-445[2]	AMPAC In-Space Propulsion	Flight qualified	1.6	0.41	Hydrazine	445	235	5.60E+06
MRE-0.1[3]	Northrop Grumman Space Technology (NGST)	Chandra X-ray Observatory, DSP, STEP 4	0.5 (STM) 0.9 (DTM)	0.175	Hydrazine	1	216	
MRE-1.0[3]	NGST	Pioneer, HEAO, TDRSS, FLTSATCOM, EOS, SSTI, STEP4	0.5 (STM) 1.0 (DTM)	0.188	Hydrazine	5	218	
MRE-5.0[3]	NGST	GRO	1.5 (DTM)	0.264	Hydrazine	36	232	
DOT-5[1]	KB Khimmash	spacecraft thruster	0.9		Hydrazine	5	230	
MR-103G[4]	Aerojet	Flight proven	0.33	0.173	Hydrazine	0.19-1.13	202-224	97078
MR-111C[5]	Aerojet	Flight proven	0.33	0.169	Hydrazine	1.3-5.3	215-229	
MR-107N[6]	Aerojet	Fligth proven	0.74	0.213	Hydrazine	109-296	229-232	68500
MR-80B[7]	Aerojet	Flight qualified	8.51	0.411	Hydrazine	31-3780	200-225	
CHT-1[8]	EADS Astrium	>500 units flown	0.29	0.172	Hydrazine	0.32-1.1 (v)	200-223	1.12E+05
CHT-20[8]	EADS Astrium	Flight proven	0.395	0.195	Hydrazine	7.9-24.6 (v)	224-230	5.17E+05
CHT-400[8]	EADS Astrium	Flight proven	2.7	0.325	Hydrazine	130-455 (v)	214-224	>5e5

Aeroiet's MR-111C

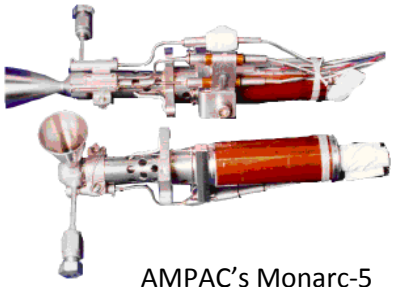

AMPAC's Monarc-5

Figure 18- 4. Typical Hydrazine (N_2H_4) Monopropellant Engines. Pictures courtesy of GenCorp Aerojet and AMPAC In-Space Propulsion respectively.

Bipropellants. In a bipropellant system a fuel and an oxidizer combust either spontaneously after they contact each other (hypergolic systems) or as a result of an ignition source. Table 18- 6 shows many examples of bipropellant engines and Fig. 18-5 shows representative engines. This type of system is much more complex than cold gas or monopropellant systems (Fig. 18-8). They are used for high ΔV requirements (>1000 m/s) [Micci and Ketsdever, 2000] and their I_{sp} ranges from about 270 to 466 s.

Both propellants undergo a series of processes from the moment they are injected into the combustion chamber to when they leave the nozzle. The propellants can be injected as liquids, vapors, or supercritical fluids (mostly the case in recent engines). Depending on what thermodynamic state they are in when they are injected and what type of injector is used, the mixing process can be very different. In cryogenic engines, for example, a shear coaxial injector is commonly used, which consists of a center tube carrying liquid oxygen and an annular tube carrying H_2. If a propellant is liquid, it has to break into droplets first, vaporize, and then mix and combust with the other propellant. If the propellants are in the supercritical phase (P >critical pressure, $\mathrm{Temperature}$ >critical temperature), no droplets are formed and the fluids mix more in the fashion of two dense gases.

There are two choices to pressurize the propellants; the simpler one is to pressurize the propellants in their storage tank by means of a high pressure inert fluid. The high pressure propellant then discharges into the combustion chamber. In this case, the storage tanks have to be designed to withstand high pressures, which requires thicker and heavier tanks. Such pressurized feed systems are usually preferred when the total impulse needed is relatively low, short periods of operation are required, and the thrust to weight ratio is low. This design is the common choice for in-space propulsion systems. Alternatively, *turbopumps* (pumps driven by turbines) can be used to pressurize the propellants. The storage tanks for the propellants don't need to withstand high pressures then. However, the pressurization system as a whole increases in complexity. Turbopumps are usually not used for in-space applications, but rather they are used for higher pressure, higher performing systems. Virtually all major boost liquid rocket engines flying today use turbopumps.

There are many different ways to configure a working cycle for a bipropellant rocket engine. For a detailed description including diagrams see Sutton and Blibarz [2010]. The cycle most used for cryogenic upper stage engines is the expander cycle. In this cycle one propellant (usually hydrogen) is first used to cool the combustion chamber, and then the heated H_2 is used to run the turbine or turbines which run

the pumps. After the warm hydrogen leaves the turbine it is injected into the combustion chamber. Some of the hydrogen goes directly from the cooling jacket to the combustion chamber. At that point, you will have liquid oxygen and warm hydrogen mixing and combusting. One limitation of this cycle is how much heat can be transferred from the combustion chamber walls to the H_2; hence an active area of research for expander cycles is heat transfer enhancement techniques. Some of the advantages of expander engines are their simplicity and the fact that no propellant is thrown overboard. This last feature makes this a closed or topping cycle. The RL-10 is the premier example of an expander cycle (Fig. 18-5). Derivatives from this engine are used on both the Atlas V and Delta IV launch vehicles. Hydrogen is particularly well suited for this application since it absorbs heat efficiently and it does not decompose chemically like heavier hydrocarbons do. As a note for the reader, for heavy hydrocarbons like RP-1 or RP-2, we have to carefully study the thermal decomposition characteristics of the fuels as they heat up while cooling a combustion chamber. If these hydrocarbons are heated beyond a certain temperature they can produce carbonaceous deposits, which can clog cooling channels and modify the heat transfer process by coating the walls with deposits.

A second cycle to consider is the gas generator cycle. In this case, some of the propellants are combusted on what is generally called a 'gas generator', a little misleading since it is in fact another smaller combustion chamber. The hot products from the gas generator drive the turbine(s) and generally they are exhausted overboard after that, which makes this an open cycle. Dumping hot gases overboard decreases the I_{sp} by about 2-5% for a given chamber pressure [Humble, 1995]. The rest of the propellants combust in the main chamber. Since the turbine is driven with combustion products, the temperature can be higher than that achieved on an expander cycle. The F-1 rocket engine which powered the Saturn V used a gas generator.

The last and most complicated cycle is staged combustion. This is similar to the gas generator cycle except that the hot products which drive the turbine are injected into the main chamber instead of being thrown overboard. Also, the gas generator usually consists of either very rich or very lean mixtures. That is, there is usually much less or much more oxidizer than needed to burn all the fuel present in the mixture, respectively. This cycle promises the highest I_{sp} and is used on the Russian RD-180 engine powering the Atlas V today.

Closely coupled to the cycle we choose are the cooling techniques for the combustion chambers. Regenerative cooling is where one propellant (usually the fuel) is passed around the nozzle to cool it, as in the expander cycle. In ablative cooling the combustion chamber walls are made of ablative materials which decompose into gases as they heat up, and these gases act as cooling for the walls. In radiation cooling, mostly used for engines operating at vacuum, the heat produced by combustion and conducted through the chamber walls is rejected through radiation. Finally, in film cooling some of the propellant is injected along the walls of the chamber, usually close to the injector exit plane and/or at the throat, and the thin film covering the wall acts as insulation. Eventually the propellant used as coolant will mix and burn but the flame temperature will be lower than that attained toward the center of the chamber since the mixture ratio will be much greater than stoichiometric.

Table 18- 6. Representative Bipropellant Rocket Systems. References: [1] Sweetman [2006], [2] Astrium [2010c], [3] Astrium [2010d], [4] Astrium [2010e], [5] Stechman [1985], Hill [1980], Sund [1979], Drenning [1978], [6] Wu [2001], Stechman [2001], [7] Stechman [1990], [8] Courtesy of AMPAC In-Space Propulsion, [9] Northrop [2010b].

ENGINE	MANUFACTURER	STATUS	ENGINE MASS (kg)	LENGTH (m)	PROPELLANTS	NOMINAL THRUST (kN)	SPECIFIC IMPULSE (s)
YF-73[1]	CALT	H-8 3rd stage CZ-3	236	1.44	LOX/LH2	44.15 (v)	420 (v)
Aestus[2]	EADS Astrium	Ariane 5 upper stage	111	2.20	NTO/MMH	29.4	324 (v)
S400-12 (-15)[3]	EADS Astrium	>60 missions flown	3.6 (4.3)	0.244 (0.292)	NTO, MON-1, MON-3 and MMH	0.42 (0.425)	318 (321)
10 N Bipropellant Thruster[4]	EADS Astrium	> 90 spacecraft have these thrusters	0.35 to 0.65	0.126-0.179	NTO, MON-1, MON-3 and MMH	0.010	291
Unified Propulsion System - Apogee Kick Engine [1]	Japan IHI company ltd	provides GEO insertion and attitude/orbit control fo 2t-class satellites	15.7	0.103	NTO/hydrazine	1.7	321.4
LE-5B[1]	Mitsubishi	H-IIA Stage 2	285	2.63	LOX/LH2	137.3/82.4 (throttled) (v)	447/448
R2.2000[1]	Russian Federation	Used on Phobos spacecraft as main engines	74	1.03	NTO/UDMH	13.73-19.61	316-325
Orbital Maneuvering System[1]	Aerojet	Shuttle: orbit insertion, manuevering, and reentry initiation	118	1.96	NTO/MMH	26.7 (v)	316 (v)
R-40[5]	Aerojet	Flight proven (Space Shuttle)	6.8	0.554-1.04	NTO (MON-3)/MMH	3.87	281
HiPAT™ [6]	Aerojet	Flight Proven	5.2-5.44	0.628-0.726	NTO (MON-3)/MMH	0.445	320-323
R-1E [7]	Aerojet	Flight proven (Space Shuttle)	2	0.312	NTO (MON-3)/MMH	0.111	280
5lb Cb[8]	AMPAC In-Space Propulsion	Flight qualified	0.82-0.91	0.216-0.270	NTO/MMH	0.022	293-295
LEROS LTT[8]	AMPAC In-Space Propulsion	Flight qualified	0.6	0.27	NTO/MMH	0.009	274
XLR-132[1]	Rocketdyne	Applicable for kick stages, deep space, space transfer vehicle	54	1.2	NTO/MMH	16.7 (v)	340 (v)
TR-308[9]	Northrop Grumman Space Technology	Flown on Chandra X-ray Observatory	4.76	0.706	N2O4/N2H4	0.472	322
Dual mode liquid apogee engine[9]	Northrop Grumman Space Technology	Canada's Anik E2/E1; telecom satellites; intelsats; 330 s version to fly on TRW's odyssey	4.8	0.561	MON 3/ hydrazine	0.454 (v)	314.5 (v)
RL 10B-2[1]	Technologies Pratt and	Delta 3 Stage 2, Delta IV Stage 2	259	4.15	LOX/LH2	105.645 (v)	466.5 (v)
RL 10A-4[1]	Technologies Pratt and	Atlas 2A/2As	168	2.29	LOX/LH2	99.2 (v)	451 (v)

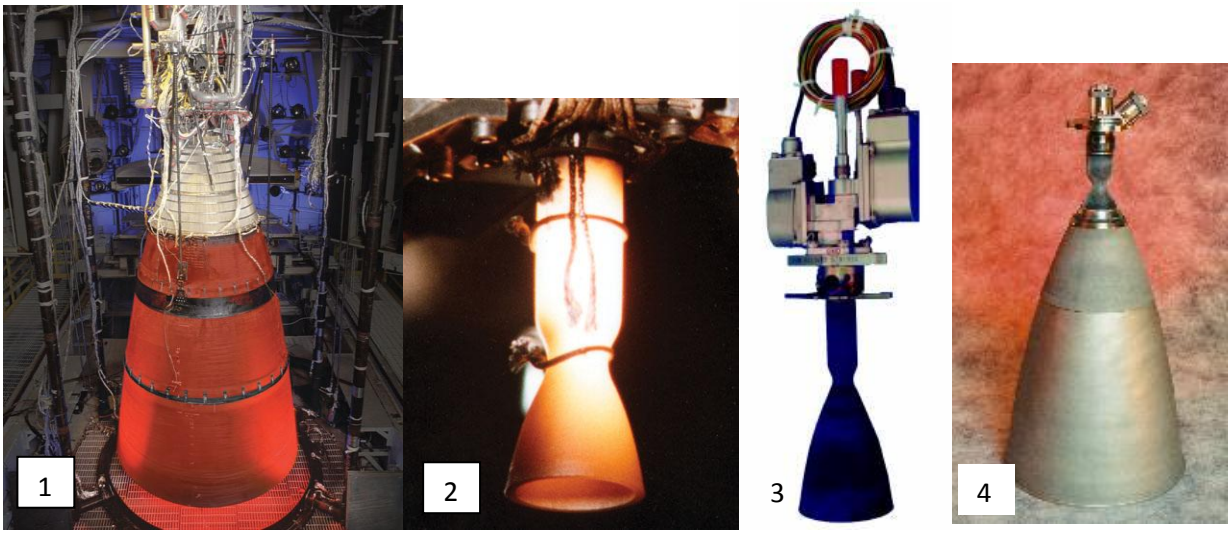

Figure 18- 5. Representative Liquid Rocket Engines. 1: RL10B-2 courtesy of Pratt & Whitney Rocketdyne, 2: KEW-7 courtesy of Pratt & Whitney Rocketdyne, 3: LEROS LTT courtesy of AMPAC In-Space Propulsion, 4: HiPAT™ Courtesy of GenCorp Aerojet.

Dual-Mode Systems. In a dual-mode propulsion system, hydrazine is used for both bipropellant and monopropellant thrusters. The hydrazine tank(s) are shared by both classes of thrusters, potentially simplifying the overall spacecraft propulsion system. Dual-mode systems also have the advantage of using the bipropellant engine for high-thrust, high ΔV maneuvers (e.g. orbit insertion, apogee circularization) and the monopropellant thrusters for attitude control. The Mars Global Surveyor, launched in 1996, used a dual-mode propulsion system [Brown, 2002] and they are still used today.

18.3.3 Solid Rockets. Solid rockets pose a major advantage over liquid rockets: simplicity. In a solid motor there are few or no moving parts (the only movable parts may be nozzles for thrust vectoring) compared to many liquid rocket engines which have complex turbopumps and feed systems. The other advantage is that solid propellants have higher density than liquid propellants so they need less volume for storage given the same mass. The propellant mixture can be stored for years inside the solid motor (like in tactical and strategic missiles). Also, the motors can be scaled up or down in thrust relatively easily, so their range in thrust varies from a few Newtons (N) to more than 1 MN. In exchange for the above advantages, solid motors have lower I_{sp}, than LOX/LH_2 engines and comparable or less I_{sp} than storable and LOX/hydrocarbon engines. Unlike liquid engines, where the propellants are admitted to the combustion chambers through valves which can be controlled, the fuel and the oxidizer in solid rockets are mixed together in what is called the propellant grain, so once combustion is established there is no mechanism to stop it. Because of that, you can neither check a solid motor performance before firing it, nor can you use one for a mission requiring multiple starts.

The main components of a solid motor (Fig. 18-6) are the case which houses the propellants and contains the pressure, the igniter which starts the combustion process, the thrust skirt to connect the motor to the rest of the vehicle, the nozzle, and a mechanism to transfer the loads from the nozzle to the rest of the motor body, usually a polar boss [Humble, 1995]. The case is lined with an insulation

layer so that the case material does not see the high combustion temperatures. The cases themselves can be metallic (e.g., Aluminum, Titanium), fully composite (e.g., carbon fiber with an epoxy resin) or composite with metal liners [Humble, 1995]. Aluminum is the most commonly used fuel today. Other potential fuels are magnesium (considered a 'clean' fuel) and beryllium (with toxic exhaust products). For oxidizers, Ammonium perchlorate is the most common, used on the Space Shuttle Solid Rocket Motors. Ammonium nitrate is the second most used oxidizer. The fuel and oxidizer are held together by a 'binder', which gives structural integrity to the fuel/oxidizer mixture (<20% of the total propellant mass) and also acts as a fuel. The binders are usually long-chain polymers [Humble, 1995]. Two common binders are hydroxyl-terminated polybutadiene (HTPB) and polybutadiene acrylonitrile (PBAN). From the data that Humble [1995] gathered, typical ranges for percentage of total mass of the different components are: 82-94% for the propellant mass, 1-6% for the insulation, 3-8% for the case, and 1-6% for the nozzle.

Solid motors are used when the total impulse required is known and they can provide from a few hundred to 10^9 N-s [Brown, 2002]. They are commonly used in the first stage of launch vehicles like the Atlas, Delta, Ariane 5, H-2 and the Space Shuttle. They provide extra thrust needed during take-off and may be jettisoned after their firing, refurbished and reused. They are also used for kick stages to GEO orbits, orbit insertion for planetary missions, and in ballistic and tactical missile systems. Table 18-7 shows applicable examples of solid motors. For example, the inertial upper stage (IUS), used from 1982 to 2004 [Isakowitz, 2004], consisted of a two-stage solid rocket motor system, an Orbus 21 motor (186 kN thrust) for the first stage and an Orbus 6 motor (76.5kN) for the second stage. The IUS placed payloads into GEO. It also placed the Magellan and Galileo missions to Venus and Jupiter, respectively, into their initial interplanetary orbits in 1989.

A very important consideration for choosing a solid motor is its total impulse capability (Eq. 18-15). Most qualified solid designs can be tailored to the specific total impulse requirements for the mission by 'off-loading' propellant. As a rule of thumb, solid motors are typically capable of offloading up to 20 % for a given design. To choose the right motor for the application at hand, one also should know how the thrust will vary as the motor fires. The burning rate of the propellants and how the combustion proceeds and the propellants get consumed falls into the realm of internal ballistics. The burning rate, r_b, denotes how much of the burning surface recedes as a function of time, usually in the order of 0.1-8 cm/s [Humble, 1995; Sutton and Blibarz 2010]. It is measured perpendicular to the burning surface. The burning rate is usually described as

$$r_b = a p_c^n e^{\sigma_p \Delta T} \tag{18-24}$$

where p_c is the chamber pressure, the pressure exponent n falls between 0.2 and 0.6, a is a constant dependant on the ambient grain temperature and the units used in the above equation. For r_b in cm/s and p_c in MPa, a range from 0.4 to 0.6 for typical motors [Sutton and Blibarz, 2010]. ΔT is the difference between the temperature at which the constant a is evaluated and the actual propellant temperature [Humble, 1995]. σ_p denotes temperature sensitivity, and it ranges from 0.001 to 0.009 1/K [Sutton and

Blibarz, 2010]. From Eq. (18-24) we see that to double the burning rate we would need to increase p_c by four times if the exponent n were 0.5. The mass being consumed by the combustion is:

$$\dot{m} = A_b r_b \rho_b \tag{18-25}$$

Where A_b is the burning area, r_b is the burning rate and ρ_b is the density of the combustion products. As the pressure increases the burning rate increases and so does the mass being burned per second and by consequence the thrust as well (Eq. 18-4). Because of this tight relation between thrust, burning rate, and burning mass, we have to be careful not to develop large cracks that propagate on the propellant grain. An unintentional or uncontrollable growth in burning area and burning rate can result in unmanageable chamber pressure rise and failure of the case.

System considerations when choosing a solid motor are 1) the need to spin stabilize the spacecraft during the solid burn (most spacecraft applications which are not upper or transfer stages) since the burning rate increases with acceleration perpendicular to its surface, 2) the thermal constraints for solid motors, paying attention to the soak back for motors which are embedded with spacecraft structures and 3) how the thrust level may affect deployables.

Table 18-7. Representative Solid Rockets. From Sweetman [2006].

ENGINE	MANUFACTURER	STATUS	ENGINE MASS (kg)	LENGTH (m)	PROPELLANTS	NOMINAL THRUST (kN)	IMPULSE (s)
Star 27 (TE-M-616)	ATK	AKM for Canada's CTS, Japan's GMS/Bs and several USAF GPS and NOAA GOES satellites	365.7	1.303	AP/HTPB/Al	27	289.5
Star 37FM (TE-M-783)	ATK	GPS	1,148	1.676	AP/HTPB/Al	47.3	289.8
Orbus 6/6E	UTC Chemical Systems Division (historic)	IUS	3018	0.198	86% solids HTPB (UTP 19360A)	81	303.5
Orbus 1	ATK	upper stages and space motor; starbird stages 3/4	470.4	0.1249	90% solids HTPB	30.4	293.3
Star 30bp	ATK	525 to increase vel of spacecraft by	542.8			1460	292

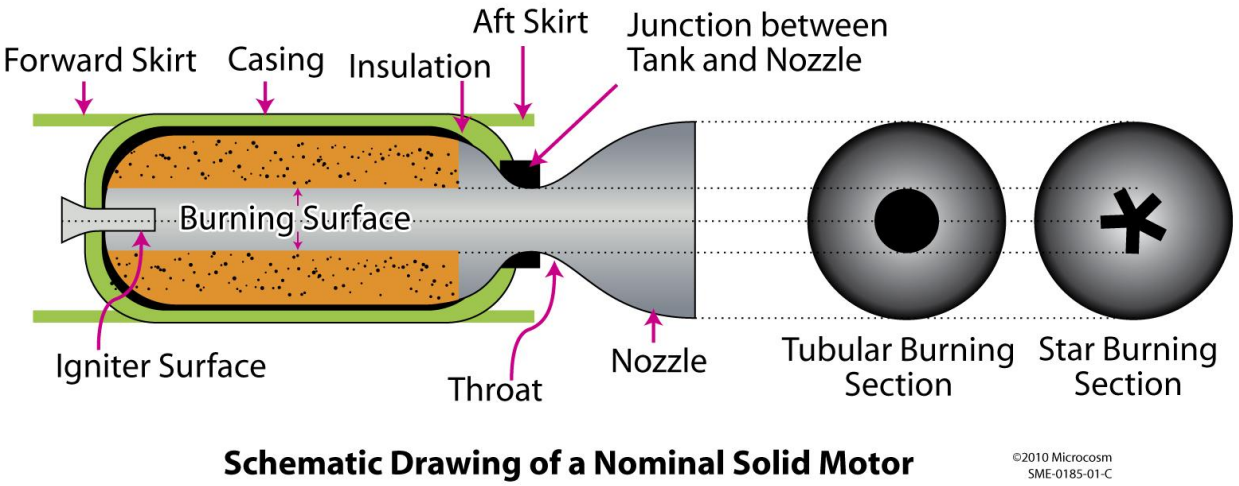

Figure 18- 6. Schematic drawing of a nominal solid rocket motor.

18.3.4. Hybrid Rockets. Hybrid rockets aim to combine some of the best traits from liquid and solid rockets. Its origins go back to Russia in the late 1930's. In a typical hybrid engine, the oxidizer is liquid but the fuel is solid. A reverse configuration is also possible. See Chiaverini [2007] for a recent very detailed description of hybrid rockets. Figure 18-7 shows a schematic description of a typical hybrid rocket. A very common fuel used for hybrid rockets is HTPB which can be used with LOX, N_2O or N_2O_4. The I_{sp} for these propellant combinations at chamber pressures of 3.45 MPa and exit pressure of 0.1 MPa are 280 s, 247 s, and 258 s respectively. If paraffin, another very common propellant, is used as fuel instead, the I_{sp} increases by 1 s for the oxidizers considered above [Chiaverini, 2007]. The potential applications of hybrid rockets span from upper stage orbital control to tactical missiles to launch systems. Some of the advantages of hybrid rockets typically mentioned [Chiaverini, 2007; Humble, 1995] are: (1) safety from fabrication to transportation to storage – unlike solid rockets, the fuel and oxidizer are stored separately so there is very little risk of a detonation or explosion; (2) higher I_{sp} than solid rockets; (3) higher density impulse than liquid rockets (but lower than that of solids); (4) ability to throttle since the thrust can be controlled by the flow rate of the liquid propellant which also results in greater maneuverability; (5) restart capability; (6) can idle the engine to check system operation prior to launch; (7) when the grain is not aluminized, it avoids hydrochloric acid or aluminum oxide exhaust from typical solid rockets so there is minimal environmental impact during launch; (8) potentially lower propulsion cost than solid and liquid rockets; (9) higher reliability (due to less parts in the system) than liquid rockets; and (10) stronger than solid-propellant grains which are less sensitive to cracks and debonds.

Even though the first hybrid rockets can be traced to the 1930's, why don't we see them occupying a prominent place in mainstream launch or spacecraft propulsion systems? Chiaverini and Kuo [2007] remark that hybrid rockets don't have the same launch readiness as solid rockets and they have lower I_{sp} than liquid rocket engines. In hybrid rockets not all the fuel is consumed, when used with liquid oxidizers, so the effective mass fraction of the solid is less than that for a solid rocket. Because the mixture ratio varies during operation, the specific impulse varies as a function of time. Regression rates

of commonly used hybrid propellants are low in comparison to solid propellants and this is an active area of research. Finally, analytical and numerical models are not as mature as those for liquid and solid rockets

In the 1980's there was a growth in commercial satellites which gave a new boost to hybrid rocket technology as an alternative for a low-cost and safe way to launch those payloads. AMROC and Thiokol had partial success with hybrid rockets but their plans to use high-thrust hybrids (1.1 MN thrust) ended in part due to combustion instability problems. A lesson learned from those experiences is that the LOX has to be completely vaporized before coming into contact with the fuel [Chiaverini, 2007]. In 2004 SpaceshipOne won the Ansari X Prize [Dornheim, 2003] using a rocket propulsion system consisting of a 74 kN hybrid rocket powered with N_2O as the liquid oxidizer and HTPB as the solid fuel. A hybrid motor is schedule to be also used for SpaceShipTwo [Norris, 2009]. Lockheed Martin launched a 267 kN hybrid rocket from Wallops, Virginia with a projected I_{sp} of 290 s in 2003 [Morring, 2003] and tested a hybrid rocket on a DARPA program in 2005 [Lockheed, 2005]. In terms of smaller hybrid rocket development, most of it is happening at the university level at places like Purdue [Tsohas, 2009], Penn State [Evans, 2009] and Stanford [Dyer, 2007].

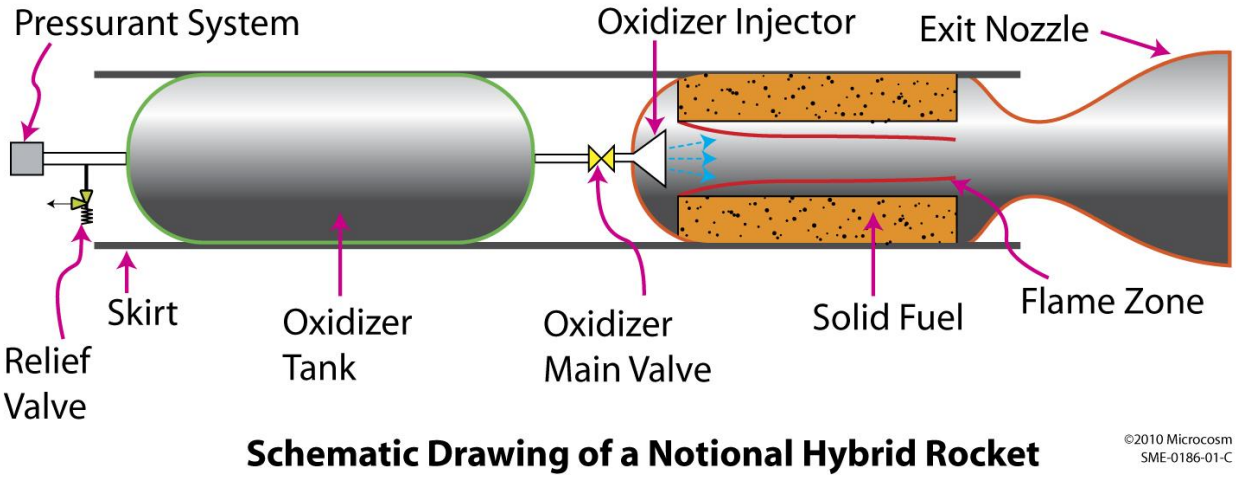

Figure 18- 7. Schematic drawing of a hybrid rocket

18.4 Plume Considerations

The plume or exhaust from a rocket is made up of combustion products, such as water vapor from LOX/H_2 engines, and sometimes also unburned propellants which can react with ambient air outside the rocket. For example, the ambient air can complete the oxidation of partially oxidized elements like CO, NO, H_2, which then go to CO_2, NO_2, and H_2O respectively. Sometimes the exhaust plume can contain toxic gases like hydrogen chloride (HCl) from the solid boosters of the shuttle. Along with HCl, nitrogen dioxide (NO_2), and nitric acid (HNO_3) make up the three major toxic emissions from common rockets [National Research Council, 1998]. An assessment of the emissions from rocket exhaust into the stratosphere is presented in Jackman [1996]. Plumes also contain solid particles like carbon soot from hydrocarbon liquid rocket engines, or aluminum oxide particles (Al_2O_3) and alkali metal impurities from

solid rockets. Al_2O_3 particles are in fact an orbital debris issue if they stay in orbit. For a detailed treatment of plumes see Simmons [2000]. For a good introduction see Sutton and Blibarz [2010].

Depending on the altitude at which the vehicle is flying (ambient pressure, p_a) and the combustion conditions of the rocket, the plume takes on different shapes. Since the area ratio and the chamber pressure usually don't change as the rocket is fired, then there is only one value of ambient pressure for which the rocket exit pressure (p_e) will match the ambient pressure. This exit pressure or altitude is a design parameter. For upper stage engines, which operate at or near vacuum conditions, the bell nozzles have much greater exit-to-throat area ratios than booster engines.

As an example, if we were to test the full nozzle of an upper stage engine exhausting to atmosphere, then for $p_a > \sim 2.5 p_e$ [Sutton and Blibarz, 2010] the flow would separate creating recirculation zones inside the nozzle. Even if the flow does not separate creating additional losses, when $p_a > p_e$ we have a loss in thrust as seen in Eq. (18-4). In this situation, the nozzle is said to be overexpanded because the nozzle was "expanded" to a value of exit pressure lower than the value of the ambient pressure (see Thompson [1972] for a nice explanation of supersonic nozzle flow regimes). A system of oblique shocks will be created to bring the pressure up to the ambient value. The initial slope of this plume is contracting. In actual flight, the plume of an upper stage engine would look very different when expanded into vacuum. At high altitudes when the exit pressure is more than the ambient pressure, the nozzle is said to be underexpanded because it did not expand down to the ambient pressure. A series of Prandtl-Meyer expansions will be setup to bring the exhaust pressure down to ambient. In this case, the plume will be expanding. When the nozzle exit and the ambient pressures match the plume has more of a cylindrical shape.

When designing the propulsion system for a spacecraft, consider where the exhaust of the plume will go. Will it impinge on critical instruments, such as cameras or other optical instruments which can be contaminated, or solar panels where it can alter the effective thrust direction? Unintended torque results if the axis of the thrust force associated with the plume is misaligned with the primary vehicle or spacecraft axes. For example, if the plume impinges on a solar panel, a force is developed (integration of the plume pressure over the impinging surface) which, when multiplied by the moment arm of the thruster to the center of mass of the spacecraft or applicable control axis, results on a torque. If such torques exist, they represent an added burden to the attitude control propulsion system which has to correct them. It is a complicated matter to predict the force the plume exerts on a surface. The analyses vary from quick estimates [Genovese, 1978] to very complicated computational fluid dynamic simulations and direct simulation Monte Carlo methods [Markelov, 2007]. The objective is to understand, among others, the spread of the plume, the chemical composition, and the velocity of the gases as they impinge a surface. In the initial design stages, a rule of thumb for thruster placement is to use a 60-degree half angle cone as a keep-out zone with the origin at the midpoint of the thruster's nozzle throat. The cone half angle is measured from the centerline of the nozzle.

Plumes can transfer significant heat to the spacecraft even if they are directed away from it. High temperature blankets or metallic heat shields are often employed to protect spacecraft surfaces from heating due to thruster radiation and plume impingement. We must consider cases in which thrusters in

close proximity fire simultaneously, as well as cases in which operating thrusters thermally affect non-operating thrusters.

The plumes are also very closely studied as identifiers for defense purposes. The emissions are mostly in the infrared range with some in the visible and ultraviolet. The specific wavelengths depend on the propellants used. For example for LH_2/LOX engines, the major plume component is water vapor which has emissions in the infrared at 2.7 and 6.3 μm [Sutton and Blibarz, 2010]. As a note, when a stage event happens and the plume from the starting stage impinges on the discarded stage, a stagnation region will be created between the two stages, and this will create a region of very high temperature which will increase the emission signal of the plume in the infrared. The plume can also attenuate radio and radar signals, so consider if the plume is on the communication line between an antenna on the vehicle and an antenna on the ground. The exhaust from solid rockets attenuates communication more than that from liquids. Finally, the plumes produce a lot of noise. The level of noise is highest close to the exit plane [Sutton and Blibarz, 2010]. We need to estimate the noise produced by the propulsion system if noise regulations need to be met.

18.5 System Design Elements

Charles M. Zakrzwski, ***NASA Goddard Space Flight Center, Greenbelt MD***

This section will cover more detailed aspects of spacecraft liquid propulsion design. Figures 18-8 a-c gives a system schematic of representative cold gas, monopropellant and hypergolic bipropellants systems. One can see the simplicity of a typical cold gas thruster which consists only of a tank, a couple of valves, a filter, a pressure transducer and a nozzle. In what follows we will focus on options for propellant storage and manifolding, pressurization systems, and other miscellaneous elements.

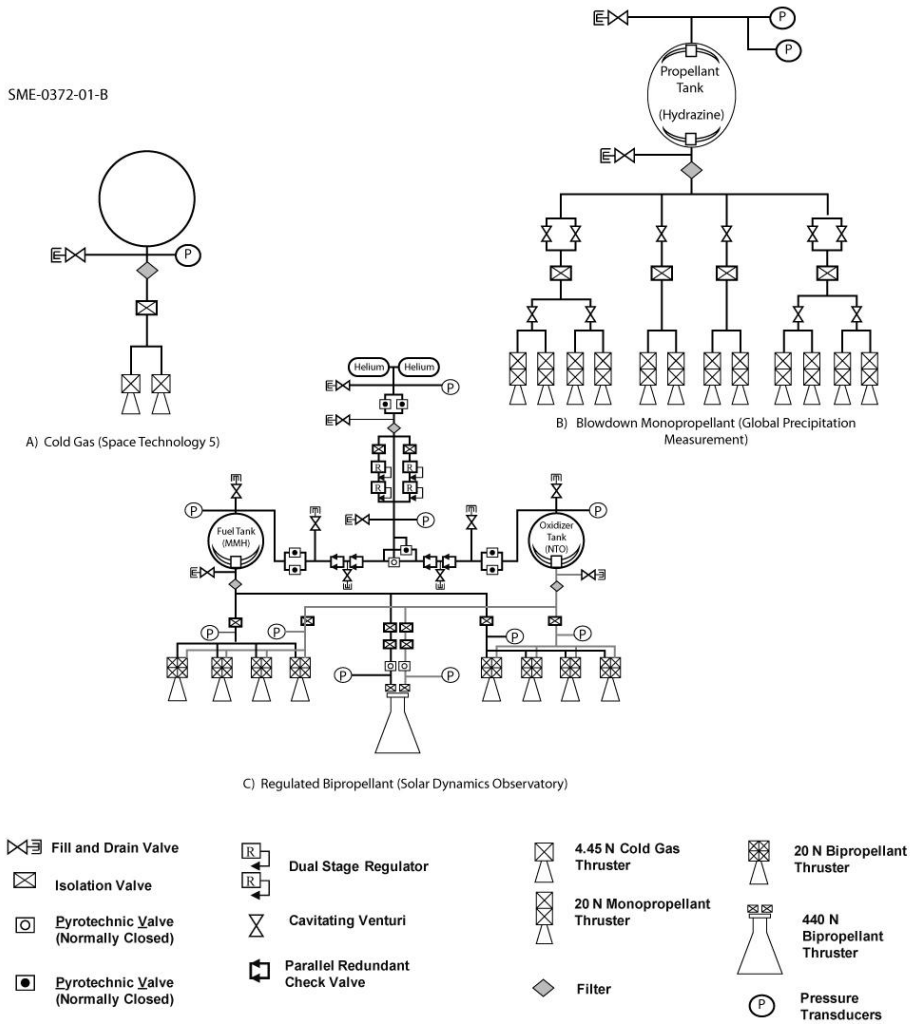

Figure 18- 8. Fluid Schematics of Spacecraft Propulsion Systems

18.5.1. Propellant Storage

Introduction. Besides thrusters, the tanks required to hold liquid are usually the most important part of a propulsion system. An ideally designed tank would have the lowest possible mass to hold and expel the required amount of propellant at the required pressure while being able to satisfy the volume and mounting constraints of the spacecraft. Because propellant tanks are pressure vessels, for mass efficiency reasons they commonly are cylindrical or spherical in shape, although ellipsoidal, tear-drop, toroidal, and other shapes have been used.

Most spacecraft propellant tanks are either all metallic, Composite Overwrapped Pressure Vessel (COPV) tanks with metallic liners, or a hybrid of the two in which only cylindrical tank sections are overwrapped. The majority of the qualified and flown metallic tanks have been constructed of titanium, though stainless steel tanks are common and aluminum tanks have also been used in a limited number of cases. The COPV propellant tanks typically have a titanium liner (although again stainless steel and aluminum have also been used) with a carbon fiber winding overwrap. Aluminum lined COPV propellant tanks

with aluminum Propellant Management Devices (see internal devices below) are being developed specifically to demise upon reentry into the Earth's atmosphere.

Integral to the choice of tanks and overall spacecraft design is the tank mounting provision. Tanks can be mounted in a variety of ways, but the most common methods are boss end mounts, hemispherical ring mounts, or circumferential skirts or tabs. Attention should be given to the most efficient way to mount the tanks so that the combined tank mass and spacecraft support structure mass are minimized. The change in tank size as it is pressurized can be significant. Usually tank mounting designs must make provisions to allow for the expansion and contraction of the tank during pressure cycles. Flexures are often used for this purpose.

Because of the amount of stored energy in both propellant and pressurant tanks, tanks are often the most safety critical component on a spacecraft, and their design, testing, and implementation are governed by several standards [AIAA, 1999; AIAA, 2006; Air Force Space Command, 2004].

Propellant tank internal devices. Devices internal to propellant tanks are used to ensure that only propellant (and not pressurant gas) is expelled from the tanks. If significant pressurant gas is sent through the thrusters, the system can lose its ability to maintain the required pressure, and thruster performance and life can be compromised. Internal fluid management devices can also act as controls on the location and movement of propellant (slosh) which can affect attitude control and act as an energy dissipation mechanism for spin-stabilized spacecraft. For spin stabilized spacecraft or spacecraft using launch vehicles with spin-stabilized stages, it is important to develop an early understanding of how the on-board propellant configuration affects what is known as the nutation time constant. The nutation time constant is the exponential constant, k, in an equation of the form: $\theta = e^{kt}$, where t is time and θ represents the nutation angle, which is the angle between the momentum vector and the coning angle. If θ grows faster than the vehicle control system can compensate, the system will be headed in the wrong direction. Baffles, vanes, screens, bladders, diaphragms, and other internal devices can be added to tanks to help control internal propellant motion, but testing is often required to prove the effectiveness of a particular design. (See discussion of LRO's nutation time constant issue in Sec. 14.6.1). Propellant slosh can also be a concern for 3-axis stabilized spacecraft. Slosh can cause pointing disturbances, and has the potential of being magnified during thruster maneuvers if the periodic thruster force is in resonance with the fluid motion.

To separate liquid propellant from pressurant gas, tanks use either physical barriers or devices that depend on surface tension. *Positive expulsion devices* include diaphragm tanks (both metallic and elastomeric), bladder tanks, bellows tanks, and piston tanks. Elastomeric diaphragms, which are internally attached around the hemisphere of the tank, are perhaps the most common positive expulsion devices because of their large cycle capability and minimal operational constraints. Disadvantages of diaphragms tanks include their higher mass and material incompatibilities with common oxidizers.

Surface tension devices internal to tanks, often referred to as *Propellant Management Devices* (PMD's), come in a variety of designs and levels of complexity. They are typically lighter than positive expulsion

devices and are compatible with most fuels and oxidizers. PMD's use surface tension forces to keep fluids separate from gases as fluid is depleted from the tank. The design of PMD's is a specialized field and can be very complicated depending on mission requirements. PMD design relies on empirical and analytical approaches. End-to-end testing of a PMD in zero gravity environments is almost always cost prohibited. Detailed design depends on the detailed mission profile.

Sizing Propellant Tanks. The tank volume required can be found from the density of propellants at the maximum expected operating temperature. The NIST webbook is an excellent resource for finding this information (http://webbook.nist.gov/chemistry/fluid/). Table 18-8 lists the density for some common propellants.

Table 18-8. Propellant Densities as a Function of Temperature

Density (g/cm^3)	283 K	293 K	303 K	313 K	323 K
GN_2 @ 27.6 MPa	0.300	0.284	0.273	0.264	0.255
Hydrazine	1.02	1.01	0.999	0.990	0.982
MMH	0.884	0.875	0.866	0.856	0.847
NTO	1.47	1.44	1.42	1.40	1.38

Knowing the propellant mass (m_{prop}) and the density of the propellant at temperature (ρ_{prop}), the required propellant tank volume (V_{prop}) can be found from the density definition:

$$V_{prop} = \frac{m_{prop}}{\rho_{prop}} \qquad \textbf{(18-26)}$$

It is common practice to have a 20% margin on propellant volume at the conceptual study phase to allow for growth in delta-V requirements, spacecraft mass growth, or other factors. As a minimum, it is wise to use at least a 5% margin to allow for the expansion of propellant due to propellant density variations as a function of temperature. For initial trade studies, the mass of a propellant tank can be estimated using empirical data from qualified tank designs. Figures 18-9 and 18-10 show graphs of qualified tank design masses as a function of volume for tanks with operating pressures between 1.4 and 3.1 MPa. These graphs can be used to estimate propellant tank mass. Note that this does not account for differences in propellant expulsion devices or mounting requirements.

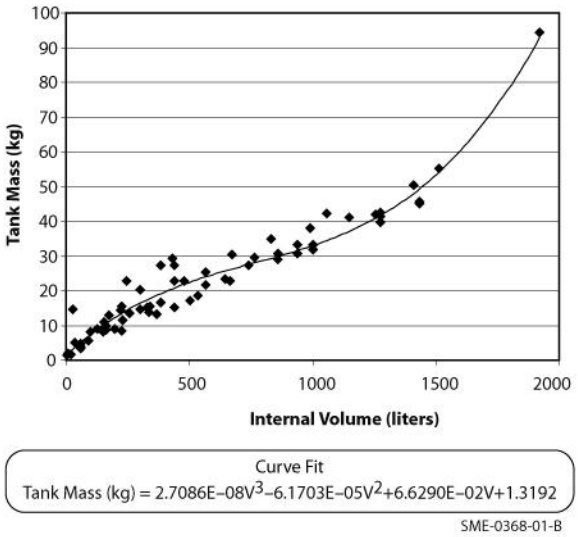

Figure 18- 9. Typical PMD Propellant Tank Mass

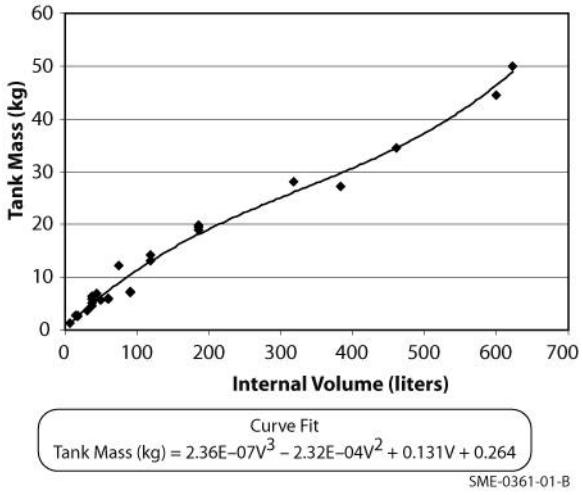

Figure 18- 10. Typical Diaphragm Propellant Tank Mass

18.5.2. Propellant Manifold

The propellant manifold (or propellant feed system) consists of all the hardware that is required between the propellant tank(s) and the thrusters. It should be noted that valves integral to thrusters are sometimes considered part of the manifold system because they are relied upon as mechanical inhibiters to thruster firing. For this reason many thrusters incorporate series redundant valves for fault tolerance. Referring to Figure 18- the various components will be discussed.

Lines and Fittings. The two most common tube and fitting materials are titanium and stainless steel. Titanium tubing is lighter and compatible with oxidizers. Stainless steel is less expensive, more readily available, and easier to weld. Fabrication of lines involves the bending, precision cleaning, and chemical

passivation of the lines. Integration of manifolds and components is performed in clean rooms to prevent any internal contamination of the propulsion systems.

Isolation Valves. Isolation valves (or latch valves) are valves that can be commanded to an open or closed position and remain in that position without continuous power. They serve several functions like providing a required mechanical inhibit between the tank and the thruster outlet, isolating groups or banks of thrusters in the event of systems failures; and isolating individual tanks in a multi-tank system in order to control spacecraft mass properties.

Pyro Valves. Pyro valves are pyrotechnically actuated, one-time-use valves. They can be either normally open (allowing flow until fired closed) or normally closed (preventing flow until fired open). They can serve the same function as isolation valves with the exception that they can only be operated once. The advantages they have over isolation valves include lower leak rates, smaller steady state pressure drop, and smaller mass. Pyro valves are often used to isolate components for safety and reliability concerns during the ground operations and launch phase or to isolate system components after they have completed their function during the mission. System implementation of pyro valves must include consideration of shock induced from activation.

Filters. The standard practice is to have propellant filters immediately downstream of propellant tanks and any fill and drain valve servicing the tank, since the majority of particulates are likely to come from the tank or fuel itself. The size of the filter is dependent on the amount of propellant required to pass through the filter, the size of particulate filtration, and the allowable steady state pressure drop. In addition to these stand-alone filters, other individual components such as isolation valves, regulators, and thruster can have integral filters. The inclusion of filters in the system does not alleviate the need to maintain strict cleanliness of the propulsion system. Particulate contamination can cause valve leakage or flow blockage that can be mission ending. Chemical contamination can lead to catalyst bed poisoning for monopropellant systems or degradation of material properties in high temperature coatings for bipropellant systems.

Fill and Drain Valves. Some fill and drain valves are used solely for functional testing of components once the systems is fully integrated. It is a standard requirement to have access to the fill and drain valves once the spacecraft is in the launch vehicle fairing to allow for emergency offloading of propellants.

Pressure Transducers. Pressure monitoring is required for propellant loading, pressurization, and ground operations. Pressure monitoring on orbit is also used to evaluate the performance of the system, to indicate possible failures, and to estimate parameters such as thrust, specific impulse, and propellant mass consumption.

Flow Control Orifices. They are typically simple, machined fittings welded in line with the system manifold. Flow control orifices are sometimes used to equalize any difference in pressure drops between fuel and oxidizer feed lines so that the ideal thruster mixture ratio is maintained. Flow control orifices are also used to minimize the transient flow in propulsion systems that can cause damaging internal pressure spikes. Pressure spikes of this nature, called *water-hammer* events are common in the

plumping and piping industry. Water-hammer events occur in liquid propulsion systems when valves command to change state. (You may have experienced water hammer in your home plumbing system if you suddenly turn a faucet on or off.)

18.5.3. Aspects of Pressurization Systems

Blow-Down Systems. A blow-down system is one in which an initial gas volume (or ullage) in a propellant tank system is pressurized to a beginning-of-life pressure and then allow to expand and decrease in pressure as propellant is consumed. This simple pressurization scheme can save on the cost and complexity of a regulated pressurization system. To use this type of system the mission must allow for the required tank volume and accommodate decreasing thrust levels as the mission proceeds Blow-down systems are more common on cold gas and monopropellant systems since monopropellant thrusters are typically qualified over a wide range of thruster inlet operating pressures (5.5 – 2.4 MPa). Bipropellant systems often have a limitation on the allowable inlet pressure range because of the need to have an acceptable fuel to oxidizer mixture ratio. Because of this, the blow-down pressure range for bipropellants is limited. It is common to have bipropellant systems start off in a pressure regulated mode and then transition to a blow-down mode once the ullage in the propellant tank is sufficient large to allow for blow-down operation.

Regulated Systems. Pressure regulated systems are, as the term implies, systems in which the propellant tank pressure is regulated at a fixed pressure over part or all of the mission life. The advantages of pressure regulated system include; maximizing the propellant that can be carried in a given tank volume, providing for consistent thrust and impulse levels, and providing consistent mixture ratios for bipropellant systems. The pressurant gas, most often He or N_2, is stored in high pressure tanks (typically at 13.8 to 41.4 MPa) and regulated to the operational pressure of the propellant tanks and/or thrusters. Regulation is performed by a mechanical regulator or, in some cases, a series of high-pressure valves commanded open and closed by a pressure feedback control loop.

Pressurant Mass Determination. To obtain a first order estimate the mass of pressurant gas and the size and mass of the high pressure tank you can work backwards from the end-of-life pressure required and total propellant tank volume. (For a detailed determination of pressurant gas mass you must consider the effects of the pressurant gas dissolving into the propellant, which is a function of pressure, temperature, and the type of fluids being used.) For a pressure regulated system, the following steps can be taken as a first approximation.

1. Estimate a maximum beginning of life operating pressure and temperature of the high pressure tank. This would be the operational design requirements for the pressurant tank. Choose 27.6 MPa at 323 K as a starting point if you have no other inputs.

2. Determine the density of the pressurant gas at this state using a lookup table like Table 18-9 or http://webbook.nist.gov/chemistry/fluid

Table 18-9. Pressurant Gas Density as a Function of Temperature and Pressure

	Nitrogen Gas Density (kg/m^3)					Helium Gas Density (kg/m^3)			
	293K	303 K	313 K	323 K		293 K	303 K	313 K	323 K
13.8 MPa	156.2	150.0	144.3	139.1		21.26	20.61	19.99	19.41
20.7 MPa	224.9	216.1	208.0	200.6		30.94	30.02	29.15	28.33
27.6 MPa	284.0	273.4	263.6	254.6		40.06	38.90	37.81	36.78
34.4 MPa	333.8	322.2	311.4	301.4		48.68	47.31	46.02	44.79

3. Assuming the ideal gas law, $PV = nRT$, for the end of life condition we can write:

$$V_{total} = \frac{m_{gas} R_{gas} T}{P} \qquad (18\text{-}27)$$

Here P is the end-of-life (E.O.L.) tank pressure, which is often assumed to be the lowest acceptable thruster inlet pressure. The pressurant gas mass, m_{gas}, is unknown. R_{gas} is the specific gas constant of the pressurant gas and is found by dividing the universal gas constant by the molecular weight of the pressurant gas. T is the gas temperature at end of life and can be assumed to be the lowest operating temperature of the tanks. V_{total} is the total gas volume of both the propellant tank and pressurant tank and can be expressed as:

$$V_{total} = V_{prop} + V_{pres} \qquad (18\text{-}28)$$

V_{prop} is the propellant tank volume which was found above in Sec. 18.5.1., V_{press} is the pressurant tank volume which is unknown. Assuming all of the pressurant gas is held within the high-pressure tank at the beginning of life (B.O.L) we have from the density equation

$$V_{pres} = \frac{m_{gas}}{\rho} \qquad \textbf{(18-29)}$$

Here ρ is the density of the pressurant gas at maximum pressure and temperature found in Step 2. Substituting Eqs. (18-27) and (18-29) into Eq. (18-28) we get the following equation for the pressurant gas mass.

$$m_{gas} = \frac{P V_{prop}}{\left(R_{gas} T - P/\rho\right)} \qquad (18\text{-}30)$$

Solve for the pressurant mass with the assumed E.O.L. tank pressure and E.O.L. tank temperature. As an initial estimate 689 kPa at 293 K for these EOL can be used.

4. Determine the pressurant tank volume from the gas density and mass (Eq. 18-29).

5. With the assumed beginning of life maximum operating pressure of the pressurant tank from step 1 and derived pressurant tank volume from step 4, the graph in Fig. 18-11 can be used to estimate the pressurant tank mass. Figure 18-11 uses this maximum operating pressure

multiplied by the volume as a way to indicate the pressurant gas mass capability of tanks. The plotted points corresponds to flight tank data with all metallic tanks represented by the x's and composite overwrapped tanks represented by the o's. A curve fit for each tank type is given to estimate the tanks mass for a given pressure-volume parameter.

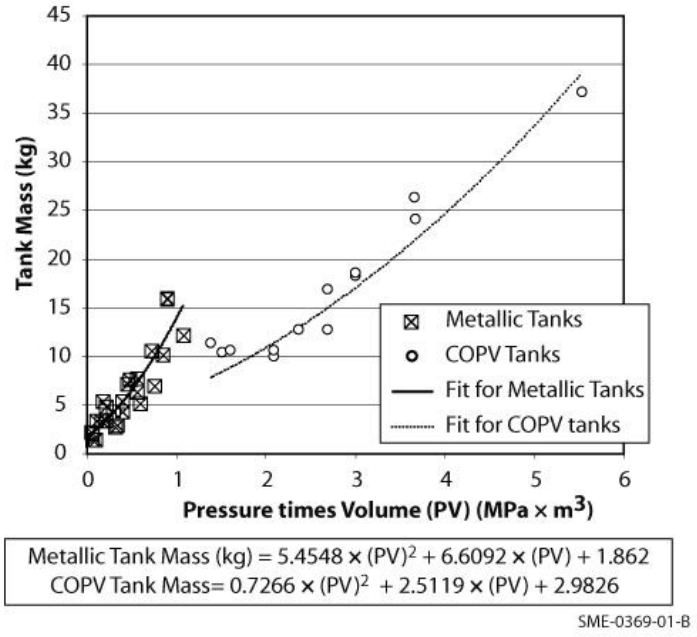

Figure 18- 11. Pressurant Tank mass as a Function of Operating Pressure times Volume

Both all-metallic and COPV tanks are included on this graph. The transition from all-metallic to COPV obviously occurs around a PV of 1.2 MPa×m^3.

Regulators. Mechanical regulators are commonly used, although as mentioned previously, electronically controlled valves in a pressure feedback system have also been used. The selection of a regulator is a function of such parameters as; the desired operating pressure, the range of flow rates required, the regulator *lock-up pressure* (the minimum downstream pressure at which the regulator closes completely), the maximum upstream pressure, and the minimum opening pressure. Another common consideration is the ability of the regulator to handle a "*slam start*" event. Slam start occurs when a sudden high-pressure surge is initiated by an upstream pyro valve or isolation valve being opened. Regulators will take time to react and the system will have a limit on the amount of gas allowed to pass downstream before the regulator reaches its normal operating condition. Also, it is a good practice not to rely on regulators to isolate high-pressure sources from low-pressure tanks over long durations (several months or greater) because of the potential for leakage. Isolation valves or pyro valve are often used instead.

Check Valves. Check valves are used to allow gas flow in one direction but prevent gas from flowing in the opposite direction. They are commonly used to prevent fuel and oxidizer vapors from migrating from the gas side of the propellant tanks and mixing with one another in shared pressurization systems.

Most bipropellants pressurize both fuel and oxidizer from a common regulated gas source in order to have a reliable mixture ratio at the thrusters. If fuel and oxidizer vapor mix, there is a strong potential for combustion which will cause catastrophic system failure.

18.5.4. Other System Considerations

Thermal Integration. Although temperature limits can vary slightly, typical hydrazine and non-cryogenic bipropellants have temperatures ranging from 281 to 323 K. Many spacecraft configurations will require that part or all of the propellant lines be wrapped with heaters to keep the propellant above a minimum temperature. Individual flow components may have heaters placed directly on them or on mounting brackets or plates. These heaters are typically etched foil elements enclosed on both sides by Kapton film. Propellant tanks are typically covered with heaters attached to the outside of the tanks. The poor thermal conductivity of titanium, stainless steel, and carbon windings drives the thermal design such that relatively low power heaters cover a large portion of the components. Often aluminum or even copper tape is used to distribute the heat from the heaters to the rest of the components. In most situations the propellant lines, components, and tanks have individual blankets. These heaters, tape, wiring and blankets can add significant mass.

Hydrazine thrusters typically require preheating of the catalyst bed prior to operation of the thruster. Catalyst bed heaters are usually heated for a predetermined time prior to thruster operation instead of relying on temperature monitoring. This power is usually book kept under the thruster's operating power instead of thermal system power.

Another thermal concern is the temperature drop due to pressurant gas expansion as propellant is consumed. This is primarily a concern for long and/or high thrust burns in which the pressurant gas is expanded at a rate that does not allow for relative thermal equilibrium between the tank and gas. It is possible for the temperature in the pressurant tanks to decrease dramatically (for example a change of over 50 K may be possible). To accommodate large burns you can start with a high initial gas temperature before the start of the burn or you can heat the pressurant gas heated through a heat exchanger before it reaches critical components.

Electrical Interfaces. Electronics are required to operate propulsion systems. Drive electronics for propulsion valves (thruster valves, isolation valves, and pyro valves) supply the appropriate power to actuate valves and account for effects such as the back EMF (Electro-Magnetic Field) seen with solenoids. Valve drive electronics are often part of the attitude control subsystem because they must work in union with the rest of the spacecraft control system. Sometimes pyro valve drivers are placed on a separate pyro valve bus with other pyrotechnic components. Power to the propulsion survival heaters often comes directly from the spacecraft power supply subsystem. Power for catalyst bed heaters and pressure transducers may also come directly from the power subsystem or from an attitude control box. Propulsion telemetry, which is primarily pressure, temperature, and valve position readings, is sometimes handled directly by the spacecraft command and data handling subsystem.

18.6 Electric Propulsion

William Hargus, *Air Force Research Laboratory, Edwards AFB, CA*

Electric propulsion traces its roots to Robert Goddard and others who independently determined that, unlike chemical propulsion, which is limited to intrinsic molecular bond energy, electric propulsion has the capability to increase specific impulse to values of 20,000 s or more [Jahn, 1968; Goddard and Penray, 1970; Choueriri, 2004]. Despite this early recognition of the potential benefits of electric propulsion, routine electric propulsion flight did not occur until the early 1990s. Although confined to low thrust applications due to limited onboard power generation and storage, electric propulsion is presently one of the more dynamic and inventive propulsion fields.

18.6.1. Classification by Acceleration Mechanism. Although there are a multitude of thruster concepts, electric propulsion may be divided into three general classes by the mechanism by which the propellant is accelerated [Jahn, 1968].

Electrothermal. In electrothermal electric propulsion, propellants are electrically heated and then expanded through a nozzle. There are several energy deposition methods by which electrothermal acceleration of propellants may be realized. These vary from relatively simple resistive heaters *(resistojets)* and slightly more complex electrical arc heaters *(arcjets)*, both of which accelerate their heated propellant through a supersonic converging-diverging nozzle [Jahn, 1968], to more exotic laser ablative thrusters, which have demonstrated that a nozzle is not necessary due to the two dimensional isentropic expansion of the superheated ablation products from a surface [Phipps, 2006].

For electrothermal thrusters, the rocket equation (18-13 and 18-18) holds and light propellants will yield the highest specific impulse. The use of propellants containing carbon and oxygen is generally avoided due to carbon deposits shorting across electrodes and oxidation of refractory metal nozzles. However, various electrodeless thruster concepts utilizing inductively coupled, or microwave resonance cavity, plasmas have been developed in the laboratory to overcome this limitation [Hruby, 1997; Balaam, 1995; Sullivan 2004].

Electrostatic. In electrostatic propulsion, electric fields are used to accelerate charged particles. The force acting on a charged particle in the presence of electric and magnetic fields is described by the Lorentz equation [Jahn, 1968; Wangsness, 1986].

$$\vec{F} = q(\vec{E} + \vec{v} \times \vec{B}) \tag{18-31}$$

where $\vec{F}$ is the force on a charged particle of charge q and velocity $\vec{v}$ produced by electric field $\vec{E}$ and magnetic field $\vec{B}$. For electrostatic electric propulsion, where there is no magnetic field or it does not contribute substantially to the propellant acceleration, Eq. (18-31) reduces to $\vec{F} = q\vec{E}$.

An interesting system level issue for electrostatic electric propulsion is that heavy propellants are preferred to light propellants. This preference stems from limited spacecraft electrical power. Using the definition of I_{sp} and defining the thruster efficiency η as the quotient of the output directed kinetic

energy flux ($\frac{1}{2}\dot{m}V_e^2 = \frac{1}{2}Tg_oI_{sp}$) and the input electrical power P_{elec} Eq. (18-32) illustrates the limiting relationship between P_{elec}, T, and I_{sp} [Jahn, 1968].

$$T = \frac{P_{elec}\eta}{2g_oI_{sp}} \tag{18-32}$$

where g_o (9.80665 m/s) is the Earth's gravitational constant, and I_{sp} is the thruster's specific impulse. Since electrical potentials of several hundred volts are required to accelerate ion beams, light ions produce very high specific impulses, but correspondingly low thrust levels at constant thruster power. High mass ions have long been used to increase thrust levels but consequently the I_{sp} is lowered. This is strongly preferred in Earth orbit where customer demand often dictates shorter orbit transfer times. For interplanetary missions, high specific impulse may alternatively be the mission enabler.

The original propellants of interest for electrostatic thrusters during early development efforts in the 1960s and 1970s were cesium and mercury, but owing to their toxicity, modern thrusters generally use xenon, although krypton and bismuth have received recent attention [Jahn, 1968; Goebel, 2008]. Electrostatic thrusters must also neutralize the accelerated ion beam to ensure the spacecraft is not charged negative by the emitted positive ion beam. Due to charge separation during acceleration by electric fields, neutralization of the ion beam is required of all electrostatic thrusters. The use of dedicated neutralizers, particularly hollow cathode electron sources, generally requires very high propellant purity (less than 10 ppm oxygen or water) in order to avoid oxidation, and subsequent failure, of the sensitive, easily poisoned electron sources.

Electrostatic thrusters may be subdivided into two categories. The first includes *gridded* and *Hall effect thrusters*. Gridded thrusters (I_{sp} = 1,500-10,000 s), often referred to as *ion engines* or *Kaufmann thrusters*, and Hall effect thrusters (I_{sp} = 1,000-3,000 s) both produce a plasma and then accelerate the positive ions which are subsequently externally neutralized. The primary difference between the two types is that the gridded ion engines produce their electric field between two, or more, very precisely aligned perforated screens, while the Hall effect thrusters magnetize the electrons in order to produce a similar, but less focused, potential difference. A more subtle difference is that ion engines produce and confine their ions non-neutrally, while the Hall effect thrusters retain a net neutral plasma during propellant production and acceleration. Ion thrusters are therefore limited in their specific thrust due to their need to contain substantial charge densities. The second subcategory of electrostatic thruster is the *electrospray* [Zeimer, 2009]. Here, ions, or in some cases charged clusters or droplets, are electrostatically extracted from an electrically conductive liquid and accelerated. Specific impulses ranging from 100 s to over 20,000 s have been demonstrated with liquids including doped glycerin, liquid metals, and various ionic liquids (molten salts). It is possible to operate these devices in a bipolar mode where the ion accelerator alternatively extracts positive and then negative ions thus eliminating the need for a dedicated neutralizer. The primary technical barrier to more widespread application of this technology has been the difficulty in scaling from microscopic single emitters to large parallelized ion extraction arrays.

Electromagnetic. Electromagnetic electric propulsion can also be described by the Lorentz equation (18-31). However, here the force on the charged particles is produced by the interaction of the charged particle velocity and the magnetic field. Since the electric field does not play a significant role in the acceleration of the plasma, Eq. (18-31) reduces to $\vec{F} = q\vec{v} \times \vec{B}$.

Electromagnetic thrusters are not as extensively developed as the other electric propulsion classes. This is due to their need for either a strong magnetic field (oftentimes heavy and complex), or high pulsed power for pulsed operation (unsteady operation). These requirements have been more difficult to accommodate on current spacecraft flown, but the electromagnetic thrusters hold promise for future high power spacecraft. On the other hand, electromagnetic thrusters can use more readily storable propellants. Light propellants, some of which are condensable and therefore more easily stored, can produce good efficiencies (>50%) as well as high specific impulses (2,000-5,000 s). Since both positive and negative particles are accelerated, neutralizers are not necessary for electromagnetic thrusters.

The two major subcategories of electromagnetic electric propulsion consist of applied magnetic field and self-induced magnetic field devices [Jahn, 1968]. However, most development has focused on self-field devices. This is due to the limited spacecraft power and mass available for propulsion that precludes heavy permanent or electromagnets. As a result, electromagnetic thruster development has, for the most part, concentrated on pulsed low-power devices with high instantaneous powers so that the requisite magnetic fields are self-generated as in the case of the *pulsed plasma thruster* (PPT) [Burton, 1998].

One significant drawback of pulsed systems is that pulse-forming networks usually rely on large capacitors. This short-term energy storage requirement makes many electromagnetic thrusters relatively high mass devices. However, scaling studies show that electromagnetic electric propulsion specific impulse and efficiency both increase with power. As a result, there is continuing interest in the development of high power electromagnetic thrusters with the assumption that electrical power levels on spacecraft will routinely reach several hundred kW in the coming decades.

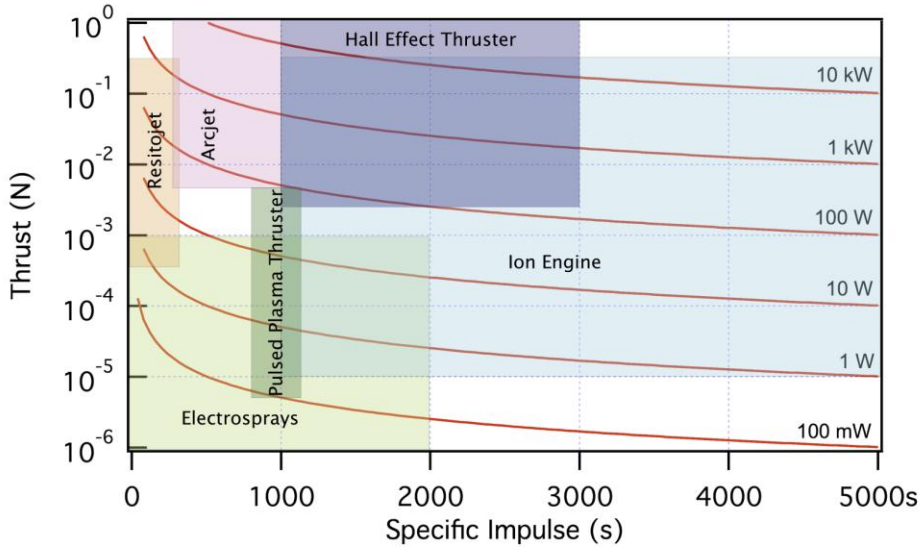

Figure 18- 12. Thruster operational envelopes with respect to thrust and specific impulse. Constant power lines assuming 100% conversion efficiency are included to illustrate electric propulsion thruster electrical power requirements.

18.6.2. Thruster Selection and Critical Subsystems. Selection of an appropriate electric propulsion thruster for any particular mission must take into account a number of important engineering constraints, including available power, mass, and volume. Furthermore, the use of electric propulsion at present constrains the mission planner to low thrust trajectories. Once all these constraints are identified and understood, a chart such as the one in Fig. 18-12 can be used to select an appropriate thruster.

It is important to note that there is considerable variability in the operating parameters (namely power) of nearly all electric propulsion thrusters. Thruster performance is usually quoted for an optimal so called *nominal condition*. Usually this condition exhibits peak electrical conversion efficiency, maximum lifetime, most stable operation, or some such combination. However, many steady state electric thrusters maybe operated between 25% and 200% of their nominal power. With special regard to electrostatic thrusters, the specific impulse can also be raised and lowered somewhat arbitrarily by varying the applied acceleration potential. It must be stressed that operation at off nominal operating parameters will likely be detrimental to the thruster electrical conversion efficiency in the short term, and lifetime in the long term. The loss of efficiency can generally be discerned from available test data, but the effect of off-nominal operation on lifetime is difficult to predict without ground test verification.

Electric propulsion systems are themselves composed of a number of subsystems. These include the thruster itself, power processing, propellant distribution, tankage, and thruster mounts (sometimes including gimbals). The most complex electric propulsion subsystem is nearly always the *power processing unit (PPU*) subsystem. The PPU regulates the spacecraft bus power and converts it into thruster required electrical potentials and currents. PPU's vary from relatively simple current sources for resistojet heating elements, several independent high voltage DC power supplies for ion engines and Hall thrusters, and extend even to high current, negative impedance arcjet power supplies coupled with pulsed arc initiation start circuits. The PPU subsystem also generally includes valve drivers for the propellant management subsystem and the digital control interface to spacecraft-based command and control.

PPU subsystems required to produce and regulate suitable electrical power for electric thrusters have finite efficiencies that strongly depend on the spacecraft bus voltage since higher bus voltages tend to increase processing efficiency. PPUs can be single set point, multiple set point, or continuously variable over some range. The addition of flexible power operation may decrease efficiencies from above 95% to below 90%. The resulting waste heat must be rejected without adversely affecting the operation of the host spacecraft. Thermal design of electric propulsion systems must be accounted for early in spacecraft design. As an example, consider the difficulties involved in safely rejecting 1 kW of heat from a 10 kW, 90% efficient PPU subsystem mounted within a spacecraft.

Although often viewed as the products of conventional electrical engineering, PPUs are usually the most expensive and massive component of an electric propulsion system. Space rated precision control of electrical power (typically 1-5 kW, but modules of 30 kW have been flown [Cassidy, 2002]) is expensive. The regular obsolescence of space rated analog and digital electronic components requires constant minor redesign and discourages low rate production of power processing subsystems as prohibitively expensive for commercial spaceflight activities.

There are a number of additional subsystems usually required for an electric propulsion thruster system. The *propellant management* subsystem transfers and regulates the flow of propellant from the propellant storage tank to the thruster. For gas fed systems, the assembly minimally consists of a pressure regulator, to lower the propellant pressure to a working pressure, followed by a flow regulator with appropriate feedback. Liquid electrothermal systems using monopropellants will add a catalyst bed to convert the storable liquid into a suitable gas.

Propellant storage is generally critical for electric propulsion, particularly electrostatic thrusters that use xenon propellant. These thrusters have high propellant purity requirements and up to now require metal lined tanks capable of withstanding approximately 15 MPa, yielding a storage specific gravity of greater than 1. For most electrothermal systems, propellant storage is a modified version of that used for hydrazine monopropellant systems. Although gimbals add complexity, electric propulsion is well suited to complex gimbal mechanisms. The low thrust levels and need to reduce the possibility of high energy plumes interacting with the spacecraft surfaces can make the added complexity worthwhile on the system level [Pigeon, 2006].

18.6.3. Existing Systems. The following section presents a listing of electric propulsion thrusters organized by thruster technology that have spaceflight experience, or substantial preparation for flight. These systems represent the bulk of flight capable electric propulsion at present. It should be cautiously noted that there are always developers with new electric propulsion concepts. While the propellant acceleration mechanism often engenders substantial research interest (and sometimes passion), the critical support subsystems (e.g., propellant management and storage, power processing.) are unfortunately often viewed as small issues to be resolved later. This is poor engineering practice and the complete propulsion system must always be considered in toto.

While most rocket propulsion texts have introductory sections dealing with electric propulsion, the content is oftentimes not up-to-date [Hill, 1992; Sutton, 2001]. While dated, Jahn's text on electric propulsion [1968] remains the most complete source on the subject. Several recent texts with updated electric propulsion descriptions are available [Tajmar 2003; Micci and Ketsdever, 2000; Goebel, 2008]. However due to the strong academic research in the field, the most recent advances are best documented in the technical literature. Most notably in the American Institute of Aeronautics and Astronautics conference proceedings and peer reviewed journals as well as the conference proceedings of the Electric Rocket Propulsion Society.

Electrothermal Systems. Electrothermal propulsion represents the vast majority of spacecraft electric propulsion heritage. Most are resistojets, but there are also a significant number of arcjets. The propellant for nearly all is hydrazine, but there are a few cases where ammonia has been used for its

higher specific impulse. The common use of hydrazine is due to flight heritage and the ease of reliable exothermic gasification through catalyst beds. Although capable of higher specific impulses (800 s versus 600 s for hydrazine), ammonia has much more limited flight experience and requires auxiliary heaters for reliable gasification. Table 18-10 presents available resistojets [Aerojet, 2003a; Surrey, 2007; Smith, 2006]. Similarly, Table 18-11 presents available arcjets [Messerschimd, 1996; Aerojet, 20003b; Aerojet, 2003c; Lichon, 1996; Cassidy 2002]. In most cases, the thrusters have flight heritage, or substantial flight preparation. With only one exception, power levels for flight proven electrothermal thrusters are below 2 kW. The sole exception is the 26 kW ESEX arcjet that flew on an experimental demonstration in 1999 [Cassidy, 2002].

Table 18-10. Resistojet nominal operating parameters.

Manufacturer	Name	Power (W)	Propellant	I_{sp} (s)	Thrust (mN)	Thruster Mass (kg)
Aerojet	MR-502A	750	N_2H_4	300	395	0.9
Aerojet	MR-502B	500	N_2H_4	300	235	0.9
SSTL	LPR	15-30	Butane/Xe/N_2	55-100	100	0.2

Table 18-11. Arcjet thruster nominal operating parameters.

Manufacturer	Name	Power (kW)	Propellant	I_{sp} (s)	Thrust (mN)	Thruster and PPU Mass (kg)
Univ. Stuttgart	ATOS	0.75	NH_3	480	115	5.0
Aerojet	MR-509	1.8	N_2H_4	502	254	5.5
Aerojet	MR-510	1.8	N_2H_4	600	258	5.6
Aerojet	LPATS	0.5	N_2H_4	475	85	4.3
Aerojet	ESEX	26	NH_3	815	2000	55

Resistojets, due to their simplicity, only offer approximately an 80 s increase in specific impulse over hydrazine monopropellants. Yet since they also use hydrazine propellant, resistojets can utilize existing qualified propellant management systems. This ease of transition coupled with their low power levels (<1 kW) have allowed this technology to proliferate widely. Arcjets have extended the electric propulsion inroads of resistojets by substantially increasing specific impulse at the expense of more complex power processing and increased power consumption. The adoption of arcjets for north-south GEO station keeping reduces fully fueled propulsion system mass to approximately 35% that of the hydrazine system it replaces. It should also be noted that alternative propellants, such as hydrogen or helium, can offer substantial improvements in specific impulse, but are not yet practical since they require cryogenic storage.

Electrostatic Systems. Goebel and Katz [2008] present the most up to date discussion on flight qualified ion engine and Hall effect thruster propulsion systems. Table 18-12 provides a listing of currently available commercial ion engines from a variety of American, European, and Asian suppliers [Goebel,

2008; Astrium EADS, 2010; QinetiQ 2004]. At present, flight proven electrostatic thrusters operate at power levels below 5 kW; however, several thrusters under development may exceed this by a factor of 4, and ground demonstrations have shown that thrusters can be easily clustered.

For these ion engine systems, system level mass can be approximated as follows. Thruster mass will scale 7 kg/kW with higher values for lower nominal thruster power levels. Propellant power management mass can be estimated to be 5-6 kg/kW for high power systems (>5 kW), and slightly higher for lower power ion thruster systems. An additional 5-10 kg must be allocated for propellant management. The propellant of all systems presented in Table 18-12 is xenon, which can be stored at pressures of approximately 13 MPa with a specific gravity near 1. Despite the high pressures, the tankage fraction is approximately 10 %. These values represent reasonable estimates at the time of this publication and may be reduced as more specialized and integrated systems are constructed. It should be also noted that a number of small ion engines (200 W, or less) have been and continue to be developed, primarily by universities [Takao, 2006; Loeb, 2004]. These are not included in Table 18-12 due to their large number and lack of flight experience. However, these thrusters may also be of interest to the spacecraft designer, particularly for small satellites.

Table 18-12. Nominal operating parameters of available ion engines [Goebel, 2008; Astrium EADS, 2010; QinetiQ, 2004].

Manufacturer	Name	Grid Diameter (cm)	Power (kW)	I_{sp} (s)	Thrust (mN)	Efficiency (%)
L3	XIPS-13	13	0.42	2500	17.2	50
L3	XIPS-25	25	2.0-4.3	3500	80-166	68
L3/NASA	NSTAR	29	0.5-2.3	<3100	<92	<61
JPL	NEXIS	65	15-25	<8500	<500	<81
Aerojet/NASA	NEXT	36	0.5-6.9	<4200	<236	<70
Qinetiq	T-5	10	0.48	3200	18	55
Qinetiq	T-6	30	5.0	4700	145	NA
Astrium	RIT-10	10	0.46	3400	15	52
Astrium	RIT-XT	21	5.0	4500	150	NA
Mitsubishi	μ10	10	0.34	3100	8.1	36
Mitsubishi	ETS-8	12	0.57	2500	22	48

Table 18-13 provides a listing of representative Hall effect thrusters from a variety of American and European suppliers [Goebel, 2008; Semenkin, 1999; Pigeon, 2006; Aerojet, 2003c; Busek, 2007a; Busek 2007b]. Of these thrusters, the SPT-100 constructed by the Russian Fakel Engineering Design Bureau (EDB) is the most widely flown and emulated. This thruster has been exported to a number of nations and is at present the most popular Hall effect thruster in orbit. Hall effect thrusters from other nations have seen more limited flight activity.

As is the case for ion engines, there are also a number of smaller Hall effect thrusters under development [Ito, 2007; Warner, 2006]. Again, these are primarily efforts of universities and other research labs. As such, they do not have support subsystems such as power processing systems or propellant management assemblies readily available. Hall effect thruster system masses may be approximated using nearly identical specific powers as for ion engine systems. Fig 18-13 shows a pair of SPT-100 on a spacecraft during assembly. Note that only the thrusters are visible and the ancillary subsystems are generally placed within the visible structure.

Table 18-13. Nominal operating parameters of available Hall effect thrusters [Goebel, 2008; Pigeon, 2006; Semenkin, 1999; Aerojet, 2003c; Busek, 2007a; Busek, 2007b].

Manufacturer	Name	Power (kW)	I_{sp} (s)	Thrust (mN)	Efficiency (%)
Fakel EDB	SPT-50	0.35	1100	20	35
Fakel EDB	SPT-70	0.70	1500	40	45
Fakel EDB	SPT-100	1.35	1600	80	50
Fakel EDB	SPT-140	4.5	1750	300	55
SNECMA	PPS-1350	1500	1650	88	55
Busek	BHT-200	0.200	1390	13	44
Busek	BHT-600	0.600	1650	42	55
Busek	BHT-8000	8.0	1900	512	60
Busek	BHT-20K	20.3	2750	1080	70
Aerojet	BPT-4000	4.5	1770	290	55
TsNIIMASH	D-55	1.3	1730	77	53
TsNIIMASH	D-110	3.0	2000	1777	60

Electromagnetic Systems. Flight electromagnetic thrusters have, with one notable exception, been limited to pulsed-plasma thrusters. PPT's, as they are commonly known, generally function by using a pulsed electric discharge across the face of a solid block of propellant. The instantaneous current is sufficiently large that a strong magnetic field is induced. Combined, the electric field and induced magnetic field electromagnetically accelerate ionized propellant with specific impulses ranging from 300 s to 50,000 s and efficiencies starting at 10% and rising substantially with specific impulse up to greater than 50% [Burton, 1998].

Table 18-14 presents a summary of U.S. flown PPT systems [Burton, 1998; Arrington, 1999; Busek 2007c]. These are listed by their spacecraft name as they have generally been single point designs for the past 35 years. The reader will notice that rather than thrust T, impulse bit ($I_{bit} = \int T dt$) is presented as the momentum flux performance parameter. Since these thrusters are by their very nature pulsed, their time integrated momentum flux (i.e. time integrated thrust) through a single electromagnetic propellant acceleration event constitutes a single impulse bit, I_{bit}. The solid propellant for all systems in Table 18-14 is polytetrafluoroethylene (PTFE, C_nF_{2n+2}) better known by the DuPont brand name Teflon. Other polymers have been examined in the laboratory, but have not proved viable.

The attraction of PPT technology to spacecraft designers has been and remains the simplicity of integration of these thrusters onto a spacecraft. The thruster does not require a propellant feed system or tankage. The only connections required to the spacecraft are bus power and rudimentary control. In the case of the MPACS PPT flown on the FalconSat-3 spacecraft, switching thruster power on and off is the control strategy [Busek, 2007c]. For a particular thruster, the impulse bit is linear with discharge energy. Another advantage of PPT technology is the very precise impulse bits achievable. As a result, the primary usage of PPTs has been very accurate propulsive attitude control. In fact, the Earth Observer 1 (EO-1) spacecraft reported that the jitter of using their PPT was approximately 10x less than using momentum wheels [Arrington, 1999].

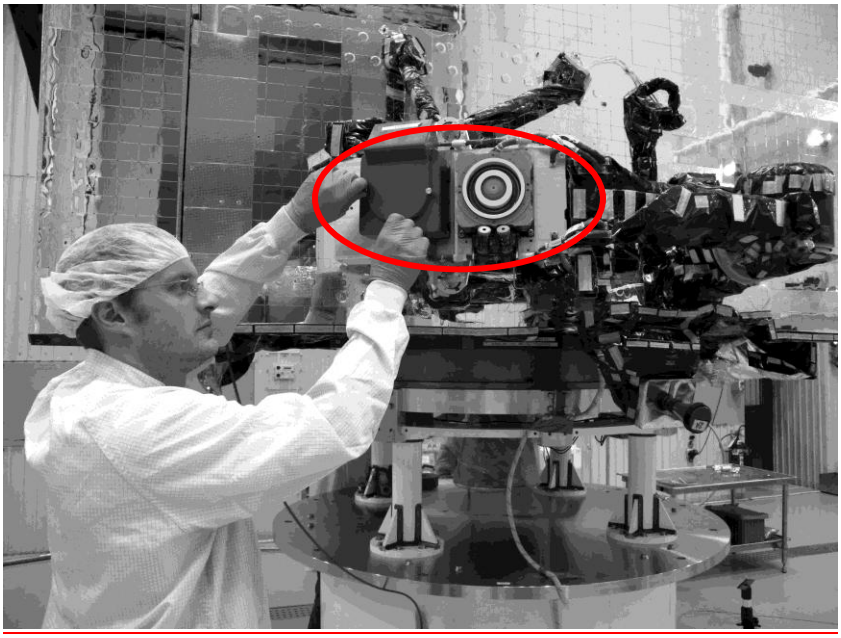

Figure 18- 13. Photograph showing a Fakel EDB SPT-100 mounted on a Space Systems Loral spacecraft under construction. Note the two Hall effect thrusters on this side of the spacecraft, one with a safety cover. Photograph courtesy of Space Systems Loral.

Table 18-14. Pulsed Plasma Thruster nominal operating characteristics [Burton, 1998; Arrington, 1999; Busek, 2007c].

Thruster Designation	Discharge Energy (J)	I_{sp} (s)	I_{bit} (mN-s)	I_{bit}/Discharge (mN-s/J)	Specific Energy (mg/J)
LES-6	1.85	300	26	14	4.8
SMS	8.4	450	133	15	3.4
LES-8/9	20	1000	297	15	1.5
TIP-II(NOVA)	20	850	375	19	2.3
MIPD-3	100	1130	2250	23	2.0

Millipound	750	1210	22300	30	2.5
EO-1	43	1136	737	60	10.0
MPACS	1.96	827	80	41	10.0

The system level mass of these thrusters can be typified by using the LES-8/9 PPT as an example [Burton, 1998]. This thruster has a total mass of 6.6 kg of which only 750 g was polytetrafluoroethylene propellant. The capacitor mass consumes an additional 1.93 kg, while the controls and structure represent the remaining 3.92 kg. Almost certainly, the non-propellant mass can be reduced with recent advances in capacitor technology and electronics, as well as in the optimization of the structural mass; however, the use of solid propellant makes the propellant feed difficult to arbitrarily expand to increase total impulse capability.

Magnetoplasmadynamic (MPD) thrusters superficially resemble the arcjets from which they were originally derived; however, they accelerate their propellant at much lower densities and to much higher exit velocities via the Lorentz force [Jahn, 1968]. MPD thrusters offer a number of potential advantages, especially at high power. They are capable of operating with large thrust densities at high power, are mechanically and electrically relatively simple, may operate on a variety of propellants (hydrazine to noble gases), and are capable of variable specific impulse. Unfortunately, MPD thruster application has been stymied by low thrust efficiencies at low power.

One experimental MPD has been flown by the Japanese space agency in 1996 [Toki, 2000]. This 43 kg demonstration MPD thruster system used hydrazine propellant and pulsed self-field configuration with a 120 μs pulse with a peak instantaneous power of approximately 720 kW and a peak current of 6 kA at a potential of 120 V (average power of 480 W). It produced impulse bits of 3.6 mN-s with an I_{sp} of 1000 s at a firing frequency of 0.5-1.8 Hz. Although a low-power flight demonstration, this experiment demonstrated the on-orbit use of pulsed electromagnetic propulsion.

18.6.4. Future Technologies. A number of electric propulsion technologies are on the cusp of flight development. Several, such as very large Hall effect thrusters, ion engines, or full sized MPD thrusters, have already been extensively developed in the laboratory and are awaiting adequate spacecraft power levels. Many other electric propulsion concepts also have a substantial pedigree, but due to various factors, these technologies have not yet been fully implemented. The amount of development to be realized for each future electric thruster depends on the tractability of the underlying physics as well as the willingness of the spacecraft community to underwrite the expense of a complete propulsion system. For successful fielding of an electric thruster, the systems must include such mundane subsystems as propellant feed and storage as well as the critical PPU system that are all too often ignored in the laboratory.

Despite having relatively low specific impulse, electrothermal propulsion remains a field of active development. Concepts being pursued include very small resistojets for use on miniature spacecraft [Ferguson, 1967; Smith, 2006]. Other technologies of interest include electrodeless thrusters, most notably propellant heating using microwave resonance cavities [Sullivan, 2004], inductive coupling

[Gesto, 2006], or laser ablation [Phipps, 2004]. The goal of these new electrothermal thrusters is to be able to use propellants with oxygen, and/or carbon that are more storable, exhibit higher performance, and are less toxic than hydrazine. There is also some discussion of multimode propulsion where a single propellant is used for both onboard chemical and electric propulsion systems, thereby providing considerably increased mission flexibility.

In addition to the scaling up of electrostatic thrusters [Jacobson, 2003], several programs are investigating boosting Hall effect thruster specific impulse above 3,000 s for interplanetary missions, primarily to take advantage of commercial Hall effect thruster system-level investments [Vial, 2009; Peterson, 2005; Hofer, 2006]. Hall effect thruster developers are also examining alternative propellants such as krypton [Linnell, 2006], bismuth [Tverdokhlebov, 2002], and iodine [Dressler, 2000].

Probably the most exciting ongoing research in electrostatic thrusters is the development of massively parallel arrays of electrosprays [Smith, 2009; Legge, 2007; Zeimer, 2009]. If the efficiencies demonstrated for single emitters can be maintained over thousands, or millions, of microscopic emitters, it may be possible to develop electrostatic thrusters of very large power levels with greater than 80% electrical efficiency over wide ranges of specific impulse, using condensed phase propellant storage. Progress in this technology lies not in improving on the physics of the propellant acceleration, but in the engineering of the parallel arrays and requisite propellant distribution system.

High power electromagnetic thruster development has long focused on MPD thrusters, which scale best for power levels above 100 kW. Metal propellants such as lithium have been proposed [Tikhonov, 1997], but lifetimes are expensive to verify and spacecraft interactions with condensable metal propellants are worrisome. Other devices such as pulsed inductive thrusters (PIT) [Mikellides, 2007], the field reversed configurations (FRC) [Martin, 2005], the variable specific impulse magneto-plasma rocket (VASIMR) [Chang-Diaz, 2000], and several other plasmoid accelerators [Choueiri, 2006; Poehlmann, 2007] are also currently being investigated as potential high power thruster technologies (Sec. 18.7.3). These systems scale well for very high power systems and are not limited by propellant selection.

18.7 Alternative Propulsion Systems for In-Space Use

Marc Young, ***Air Force Research Laboratory, Edwards AFB, CA***

Research and development is very active in the space propulsion field in general: flight qualified propulsion systems are continuously being improved; steady research is being conducted on alternative, but not yet adopted, propulsion systems, and entirely new types of propulsion systems are being investigated. It is useful to stay up-to-date on propulsion research because significant developments in either space access or in-space propulsion systems may enable entirely new classes of space missions. This section will summarize the current state of development of in-space propulsion systems as of 2010.

The state of development of emerging propulsion technologies is commonly measured relative to the DOD or NASA Technology Readiness Level (TRL) defined in Chap. 11. This section will focus primarily on the most fundamental characteristics of propulsion technologies with intermediate TRLs, 3 - 6.

In-space propulsion systems are, in general, physically smaller than space access systems and are applied to a much broader range of applications which leads to a much wider range of useful technologies. A primary difference is the inclusion of electric propulsion systems which have significantly higher specific impulses at significantly lower thrust levels. Development continues on the entire range of systems and only a very brief review can be given here.

It is reasonable to assume that the current state-of-the-art for in-space propulsion systems will continue to improve through improvements in available materials, wider operating ranges, increased lifetimes, and new propellants. This section will instead focus on new ways of propelling moderately sized spacecraft (m = 500 kg - 10,000 kg) and summarize leading candidates for both small spacecraft (m < 500 kg) propulsion systems and large spacecraft (m > 10,000 kg) propulsion systems.

18.7. 1 New Propulsion Systems for Moderately Sized Spacecraft

A variety of high performance chemical and electric propulsion systems for moderate-scale satellites have been developed. Chemical propulsion systems with ever higher energy density are being investigated. Existing moderate-scale electric propulsion systems provide a nearly complete set of consistent high performance devices except, perhaps, at a specific impulse of around 1000 s where both electrothermal and electrostatic/electromagnetic systems typically have unacceptably low efficiencies. This section discusses several representative propulsion systems that operate significantly differently than existing systems and may find use in niche applications.

Solar Thermal Propulsion. One potential method of achieving high thrust efficiency at specific impulses around 1000 s is *solar thermal propulsion* [Henshall, 2006]. Solar thermal propulsion absorbs direct solar energy with a heat exchanger. A propellant gas, typically hydrogen, flows over the heat exchanger and is expelled out of a nozzle to produce thrust. The technology has been under development for decades and may also find use in small satellite propulsion systems. Designs for solar thermal propulsion typically yield specific impulses between 400 s (ammonia) and 1000 s (hydrogen) and operate at heat exchanger temperatures of 2000 K to 3000 K. Long term hydrogen storage is still a problem that requires addressing for many systems. Dual mode systems (both power and propulsion) using significant thermal energy storage may bypass the need for photovoltaic cells and electrochemical batteries entirely. The basic technology for solar thermal propulsion systems is proven and could be employed in microsatellites in the near-term.

Solar Sail

Richard Van Allen*, Microcosm, Hawthorne, CA*

The concept of utilizing light pressure as a means of space propulsion is attributed to Konstantine Tsiolkovskii [1921], 5 years before Robert Goddard launched the first liquid-fueled rocket. Tsander [1924] coined the term "solar sailing" in the first technical publication on this topic. In that paper, Tsander calculated several interplanetary trajectories for solar sail spacecraft and identified several useful configurations. It wasn't until the 1950's that additional papers were published [Wiley, 1951; Garwin, 1958]. Leap forward 20 years to the 1970's before the possibility of rendezvousing with Halley's Comet triggered more analyses of solar sail applications (Wright, 1974, 1976; Friedman, 1978).

About the same time that the U.S. dropped trying to advance solar sail technology, a non-profit organization called the World Space Foundation was formed to promote a range of space related areas, among them advancing solar sail technology. During the period from 1977 to 1986, organization volunteers built 2 square solar sails, 225 m^2 and 900 m^2, respectively, and performed a ground deployment demonstration of the 225 m^2 sail in 1981 ["Solar Sail Unfurled," 1981]. A serious effort was initiated to perform a Space Shuttle deployment demonstration of the 900 m^2 sail, but it was shut down as a result of the loss of the Space Shuttle Challenger in 1986.

The Russians actually succeeded in deploying a 20-meter diameter spinning mirror from a Progress resupply spacecraft in 1993 that was called Znamya 2 (intended as an experiment to beam solar power to the ground, but unfurled in a way similar to how a solar sail would unfurl). However, a follow-on 25-meter diameter mirror failed to deploy in 1999 ["Projects, Organizations, and Missions," 2002]. The Planetary Society continued the hardware efforts begun by the World Space Foundation and with private funding built and attempted to launch Cosmos 1 in 2001. Unfortunately, the suborbital demonstration flight failed due to a launch vehicle failure ["Cosmos 1: The First Solar Sail," 2002]. A second attempt, this time for an orbital demonstration, also was unsuccessful because of another launch vehicle failure. In 2010, after nearly 90 years, the Japanese launched a solar sail spacecraft (Ikaros) as a secondary payload on an interplanetary mission to Mercury that validated what until then had been the theoretical ability of a solar sail to change its attitude in a controlled fashion and to change its acceleration. Now that the theory behind solar sailing has been validated, there are exciting and practical applications for solar sails that can become reality in the next 10 years. These missions include levitating payloads above and below the equatorial plane at geosynchronous altitude to make more efficient use of that crowded region and positioning payloads in "stationary" orbits above the poles for other interesting missions.

Technical Basis and Solar Sail Designs

Solar sailing **does not** involve the conversion of light into electrical energy (via solar cells), and **does not** utilize the transfer of momentum from solar wind (ionized particles ejected from the Sun) – due to the low density of the ionized particles, whose effect is < 0.1% that due to light pressure. Solar sailing **does** utilize the energy and momentum from light. The reflection of sunlight on a mirrored surface causes a change of momentum that is continuous, and the amount of "propellant" is limitless. Effectiveness falls off as the square of the distance from the Sun, so that solar sails are most effective for missions out to about the orbit of Mars.

Light-generated thrust can be used to raise or lower an orbit altitude relative to any celestial object (e.g., Sun, planet, Moon, asteroid, comet), by inclining the sail to direct the component of thrust parallel to the orbit velocity vector. If the thrust is in the direction of the orbit velocity vector, posigrade thrust raises the orbit; if the thrust is in the opposite direction, the retrograde thrust lowers the orbit. Fig. 18-14 provides an overview of the geometrical relationship of solar sail orientation relative to the incoming light (shown orbiting the sun, but the vector relationship also applies to a solar sail orbiting a planet), and Fig. 18-15 is an expanded view of Fig. 18-14 that provides the details associated with the defining solar sailing equation below (Eq. 18-33):

The thrust, F, on a flat solar sail is perpendicular to the surface of the sail with a magnitude given by

$$F=(2RSA/c)\sin^2\theta \qquad (18\text{-}33a)$$

$$= 9.113 \times 10^{-6} (RA/D^2) \sin^2\theta \qquad (18\text{-}33b)$$

where, in the second form, F is in Newtons, R is the fraction of incident (maximum of 1) light reflected by the sail, D is the distance from the Sun to the solar sail in AU, S is the solar flux, A is the sail area in m^2, c is the speed of light, and θ is the sail tilt angle – the angle between the Sun-Earth line and the sail. Equation 18-33a doesn't take into account all the factors that translate into the force resulting from light pressure because solar sail performance

involves more than the single reflectance factor, Forward [1989, 1990] analyzed the effects of various optical properties on realistic "grey" solar sails that have finite transmittance and absorptance and non-perfect reflectance, which was further broken down into specular, diffuse, and back reflectance.

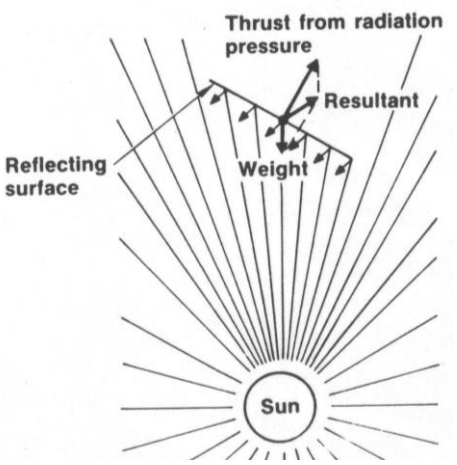

Figure. 18-14. General Depiction of How Solar Sails Maneuver.

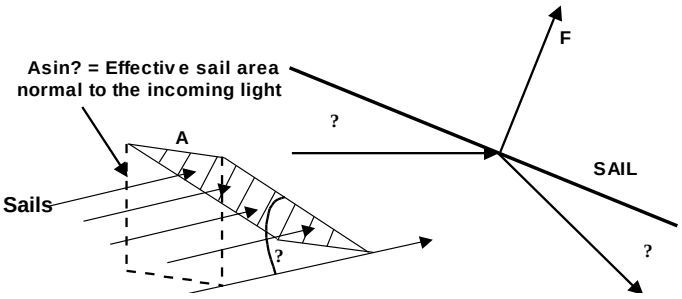

Figure. 18-15. Defining Solar Sail Equation Geometrical Relations

Figure 18- 14. General Depiction of How Solar Sails Manuever

Figure 18- 15. Defining Solar Sail Equation Geometrical Relationships

There are several factors to consider when designing a solar sail, starting with the decision on the sail material, including reflectivity, fragility, and lifetime. Aluminum is the best material because of a combination of its high reflectivity (86% - 97% for wavelengths from about 0.2 to 1.5 µm) and low density (2.70 g/cm^3) compared to gold (reflectivity 20% - ~100%, 19.32 g/cm^3), silver (reflectivity ~ 0% - ~100%, 10.49 g/cm^3), and copper (8.96 g/cm^3). At the thicknesses involved, all candidate backing materials are fragile, but rip stops can be incorporated to mitigate tearing, which is most likely to occur during deployment. Typically, the aluminum would be coated onto a backing material. Two candidate backing materials are Mylar® and Kapton®, but Mylar® degrades when exposed to ultraviolet light, so Kapton® currently is the better material.

Because solar sails for practical multi-hundred kilogram payloads could have dimensions of several kilometers, saving mass is a critical factor, even for such thin material. One option would be to coat the aluminum film on a polymer substrate that breaks down in ultraviolet light, leaving just the aluminum film (so Mylar® might actually be better than Kapton® in this case). Another interesting option for mass reduction that would make sense for very large solar sails, in the square kilometer range and larger, would be to perforate the sails with holes that are smaller than the wavelength of light (< ≈ 650 nm), which could reduce the solar sail mass by a factor of about 8 [Forward, 1984]. A third option to consider would be aluminum coated carbon fibers.

There are 3 fundamental solar sail designs: square (3-axis stabilized), circular, heliogyro (multiple "helicopter blades"). For the three-axis stabilized configuration, booms are required to support the sail material. Boom material options include composite, open truss, and inflatable structures. The 4-boom version is the most structurally efficient, but there are significant mass and deployment reliability implications associated with this configuration. For attitude control, a combination of tip vanes that are essentially miniature solar and a moveable

center of mass can be used. The circular configuration requires movement of the center of mass relative to center of pressure to maintain control and may have lower mass than the heliogyro. The heliogyro configuration requires substantial edge tendons along the blades to withstand centrifugal forces. The deployment is simpler than for the square sail configuration, but this configuration is not as mass efficient as a square sail. Relative to control, the heliogyro requires rotation to maintain stability, and the blades can be changed in pitch to control the rotation rate and attitude.

Solar Sail Applications

Independent of the particular design of a solar sail, Table 18-15 lists advantages and disadvantages of solar sails.

There is a wide range of missions that can benefit from the use of solar sails, as indicated by Table 18-16. Included are Earth-oriented missions, missions to the moon and planets, and supply/resupply missions in support of human missions to the Moon and Mars.

Table 18-15. Solar Sail Advantages and Disadvantages.

ADVANTAGES
Not propellant limited, as is the case for chemical, electric, and nuclear
Can achieve orbits not achievable by any other means or achievable only to a limited extent (e.g., cylindrical orbits, retrograde solar orbits)
Permits efficient use of geosynchronous altitude by allowing stacking of multiple satellites at the same longitude
Can perform dual roles [applies to, for example, transfers associated with going to and from geosynchronous Earth orbit (GEO) or transfers to and from another planet]:
- Boost payload to desired orbit and maintain orbit - Boost payload to desired orbit, drop it off, and return for another payload
Minimal to no orbit debris
- Can return payloads for repair - Can place payload on trajectory to burn up in the atmosphere or boost it into a safe orbit
Very large, thus very visible
For comparable missions, fewer spacecraft required (e.g., GEO communications satellite, see Fig. 18-16 – levitated orbit allows cross pole communications with 2 spacecraft instead of 3 needed to send signals “around” the geosynchronous belt)
DISADVANTAGES
Very little operational experience when compared to chemical or electric propulsion
Complex deployment, independent of configuration
Requires continuous control to maintain desired orientation
Main benefit for inner planet missions (similar to solar electric)
Vulnerable
- To attack - From orbital debris - From micrometeorites
Long time required to spiral out to desired orbit when compared to other propulsion technologies, such as chemical and nuclear (for interplanetary missions, an option is to use chemical propulsion for Earth escape)
Very large, thus very visible
Higher performance versions require space fabrication

Table 18-16. **Solar Sail Mission Candidates**.

EARTH ORIENTED	**SPACE EXPLORATION**
<u>Commercial/Scientific</u>	Solar – especially very high latitude
Weather	Retrograde orbit missions (e.g., Halley comet

Communications Miscellaneous - Solar storm warning - Payload repair/replacement <u>Government/Military</u> Weather Communications Surveillance, especially at high latitudes – optical, signals Satellite Inspection/Negation (i.e., anti-satellite) Orbit transfer vehicle – transport payloads to/from desired orbits	rendezvous) Inner planets – Venus, Mercury, Earth, Mars Human mission supply/resupply – moon, Mars Outer planets – combine sail capabilities with gravity assist Interstellar missions – use gravity assist from close flyby of the Sun to accelerate sail to solar system escape velocity; replace solar light source with laser source to push sail

Regarding the disadvantage listed in Table 18-15 associated with chemical and nuclear propulsion, this one needs some amplification and expansion because the disadvantage is not necessarily a true disadvantage. Regarding flight time, as solar sail technology improves, and assuming for interplanetary missions that chemical propulsion is used to achieve Earth escape, absolute flight times can approach achievable flight times possible from chemical propulsion. McInnes [2004] in a figure originally created by NASA/JPL provides data on flight times to Mars. From that figure, the minimum flight time to Mars for a solar sail capable of achieving an acceleration of 1 mm/s^2 is 370 days (+ about 100 days for capture and spiral down to a useful altitude). The corresponding minimum energy (chemical propulsion) coplanar Hohmann Transfer time to Mars is approximately 259 days. The characteristic Hohmann Transfer is representative of a flight time to Mars, but is not what realistically would be implemented. However, if the launch date is missed (as was the case for the Mars Science Laboratory mission to Mars), the impact will be a wait of 780 days for Earth and Mars to be aligned for another Hohmann Transfer trajectory flight opportunity.

There are 2 Earth-oriented missions that are particularly fascinating, are extremely challenging technologically, and demonstrate the unique capabilities of solar sails. One will be discussed in the paragraphs that follow, while the other will be contained in a more complete discussion of solar sails that will be available on the web. They were chosen also because of the increased focus on the utilization of space to better understand the Earth's environment that is certain to be an area of continuously increasing interest over time. Both of them were devised by Forward. In the first instance, solar sails can use light pressure to *levitate* a payload (e.g., communications) above or below the geosynchronous plane and maintain it there indefinitely **at a fixed longitude, called a** *cylindrical orbit* [Forward, 1984, 1990]. More specifically, a levitated orbit allows continuous communications with and/or observation of latitudes not possible with equatorial geosynchronous satellites or with high inclination low altitude satellites. Even more intriguing, but technologically extremely challenging, for levitation distances > 1 Earth radius, only 2 satellites are required for cross-Earth communications (180 deg separation), rather than the three minimum required for geosynchronous equatorial communications satellites (120 deg separation).

In the second instance, a solar sail maintains its position over a pole and can provide continuous service (e.g., broadcast, data transmission, weather services, and various types of observation) to any region on the Earth, including polar regions, with only 1 spacecraft, called a *statite* orbit – [Forward, 1989, 1991, 1993]. See the website for a more extended discussion and sample calculations.

Looking at levitated orbits using non-perforated sails (i.e., sails whose sail material does not have perforations that are smaller than the wavelength of light, but which have a significant impact on reducing the mass of the sail), levitation distances of practical payloads are limited by total sail and payload mass. However, performance is still sufficient to allow stacking of communications satellites with separations sufficient to avoid signal interference and essentially eliminates the problem of crowding of the equatorial plane. Perforated sails significantly alleviate the limitations of non-perforated sails so that practical payloads become possible and also permit additional stacking.

Fig. 18-16 illustrates the overall levitated orbit geometry. The maximum altitude achievable, Z (km) is provided in Eq. 18-34a and is a function of the tilt angle θ (Eq. 18-35), that results in the maximum force normal to the equatorial plane, F_P; and is inversely proportional to the sail mass m (kg) to sail area A ratio. The tilt angle is the angle between Sun-Earth line and the sail as a function of ϕ, the angle between Sun-Earth line and Earth's equatorial plane, both angles measured in radians. The other parameters shown are considered to be constants. Besides R, S, and c, already defined, there are the constants r, the geosynchronous radius (m); G, the universal gravitational constant (m^3/kgs^2); and the mass of the Earth, M (kg).

Live Calc

$$Z = [[(2RSr^3)/(GMc)]\sin^2\theta\cos(\theta - \phi)][1/(m/A)] \quad (18\text{-}34a)$$

$$= [1714\sin^2\theta\cos(\theta-\phi)][1/(m/A)] \quad (18\text{-}34b)$$

$$\theta = \text{atan}[[3\tan\phi + \text{sqrt}(9\tan^2\phi + 8)]/2] \quad (18\text{-}35)$$

Note that there is an equatorial component to the force (not shown in Fig. 18-16, but parallel to the Earth's equatorial plane). It is much less than the gravitational attraction of the Earth, but it does have the effect of displacing the near-circular orbit to the side of the Earth away from the Sun. As is the case with current GEO satellites, it will be necessary to separate solar sail spacecraft that will be stacked at the same longitude, which means that Z for each will have to be held relatively constant throughout the year. To maintain a constant Z, the tilt angle, θ, will have to vary from the value that results in the maximum force normal to the equatorial plane, which means that the sail angle will have to be trimmed over time.

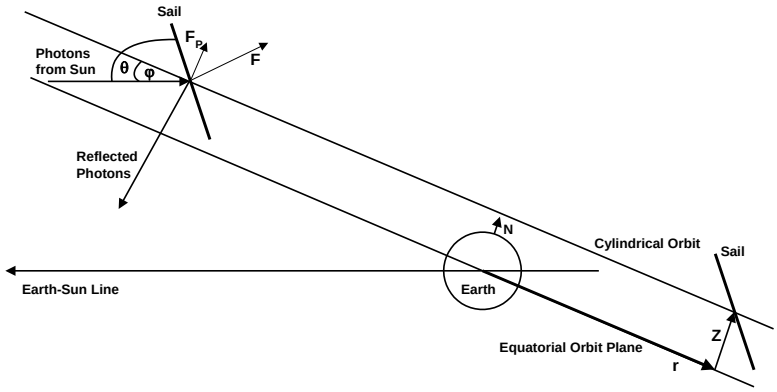

Figure 18- 16. **Levitated Geosynchronous Orbit Overview and Detailed Geometry.**

If the above equations are applied to a sail whose mass is assumed to be equal to its payload/bus mass, levitation distances vary between 50 km and 11,000 km as the sail thickness varies from 1 μm to less than .01 μm. (0.5 μm translates into a levitation distance of 150 km, and 0.02 μm represents the practical limit to sail thickness) Note that the minimum physical satellite separation at GEO is about 0.2 deg or 150 km, and in a few cases even 0.01 deg [Hudgins, 2002, UCS Satellite Database, 2010]. The payload mass is assumed to be the same as the total spacecraft

mass for a GEO satellite, since the Sail/Payload/Bus will still require such subsystems as solar cells for power and a communications subsystem. Launch masses for GEO satellites range from about 1,000 kg to 6,500 kg [Union of Concerned Scientists (UCS) Satellite Database, 2010]. Assuming no change in launch capability would imply a maximum bus/payload mass of 3,250 kg, which is what has been chosen. Clearly, very large sails are required.

There are some interesting general operational issues/challenges associated solar sails in general and with each of these orbit types in particular. In the general category, reflection from the sails is not specular since the sail material is not a perfect reflector. Hence some light is absorbed and some light is transmitted through the sail material. Also, the sail is not perfectly flat. In the case of the levitated orbits, 2 times/day the sail is approximately edge-on to the Earth so that there is potential communications impairment due to the physical blockage of the spacecraft antenna by the sail itself. Candidate solutions to this situation include cutout in the sail to permit an unobstructed communications path and putting the antennas on the tip vanes (at least for square sail configurations). Additionally, 1 or 2 times/year the sail is shadowed by the Earth once/day at all levitated altitudes that are less than about 4 Earth radii. The worst case time in the shadow is about 70 minutes, during which the levitated altitude decreases by about 5%, which is not a major impact. Besides the long round trip light time of several seconds previously mentioned, another operational issue for stationary polar orbits is the need for a clock drive for the ground station antennas. However, the electronics are still relatively simple because the spacecraft remains at almost the same range.

Finally, there are some regulatory issues to consider, in particular for the levitated orbits. Since multiple satellites can be stacked at the same longitude, some regulation will be required relative to stacking separation distances. Related to the stacking issue is who will control the physical separation of the satellites at a particular longitudinal location to ensure that separation distances are maintained. Finally, as is already the case, care will be needed to avoid communications interference.

A number of enabling technologies required to field a functionally useful solar sail are listed in Table 18-17.

Table 18-17. Enabling Technologies and Related Events.

SPACE FABRICATION - Sail material - Supporting structure/deployment methods
CAPABILITY TO REPAIR/UPGRADE SPACECRAFT - Periodically replace part or all of sail - Perforated substituted for part or all of non-perforated sail material - Carbon fiber replacement for aluminized Kapton
UPGRADE/REPLACE PAYLOADS - Change of mission - Take advantage of technology improvements – continued advances in electronics will cause payload components to shrink in mass/volume, while capabilities increase

Solar sails can perform unique scientific, commercial, and military missions, and the stage is set for near-term space missions to validate deployment and control methodologies. Enabling technologies are still required to permit high performance missions (e.g., levitated geosynchronous, stationary polar).

Momentum Exchange. Traditional propulsion systems generate thrust by accelerating propellant and ejecting it from the spacecraft. The useful lifetime of the propulsion system is completed once the store of propellant has been exhausted. For a limited class of missions (certain formation flying missions with satellite spacing of 10s of meters to over 1 km) it is conceptually possible to either bounce the propellant (in the case of light) [Bae, 2008] or collect the ejected propellant and reuse it (in the case of droplets) [Joslyn, 2010] between multiple satellites. In GEO the required thrust forces for such applications are typically between 20 and 100 mN (1 km), while in LEO it is 100 to 1000 mN.

Liquid droplet propulsion systems send a stream of liquid droplets between two spacecraft to maintain a separation force between them. One recently investigated concept uses a stream of low vapor pressure silicon oil droplets between two satellites to produce thrust [Joslyn, 2010]. The droplet propulsion system requires an order of magnitude less mass than traditional electric propulsion systems and two orders of magnitude less power to accomplish this limited role. The liquid droplets typically have diameters < 1.5 mm, speeds of about 5 m/s, and are fired at a frequency of about 0.5 Hz.

The highest achievable specific impulse is produced by photon emission: $3x10^7$ seconds. Photons are not regularly used for propulsion because the power/thrust is prohibitively high. A *photonic laser thruster* investigated by Bae [2007], however, bounces the laser multiple times between the emitting craft and a reflector on the satellite that is being accelerated. The laser gain media is in between two mirrors (one on each satellite) effectively creating a laser cavity in the entire gap between the two satellites. Proof-of-concept experiments using mirrors with a reflectance of 0.99967 achieved a thrust amplification factor of approximately 3000x achieving a thrust per unit power of approximately 20 mN/kW. Using a higher reflectance mirror (R = 0.99995) a total thrust of 1.34mN could be generated with 10W (134 mN/kW). The maximum separation that can be maintained between the two surfaces is estimated to be 1000 km.

Both classes of momentum exchange propulsion systems are at a relatively low level of development and would require significant developmental efforts to yield flight-ready systems. It is unlikely that the technology could be ready for application in the near-term.

18.7.2 Propulsion Systems for Small Satellites

Satellites with practical functionality are being constructed with ever decreasing dimensions. The classes of small satellites are discussed in Sec. 2.1.8 and smallsats and cubesats are discussed in Secs. 25.3 and 25.4, respectively, so only relevant propulsion systems will be discussed in this section. Propulsion systems are advantageous at all size scales and propulsion systems are being investigated for the entire range of smallsats. Microsatellite propulsion requirements vary significantly, but often times require very low impulse bits, high thrust levels, high thrust to noise levels, and significant ΔVs.

Solid and liquid chemical propulsion systems are being developed along with electrothermal, electrostatic, and electromagnetic electric propulsion systems. The following discussion will focus primarily on propulsion for microsatellites, or *micropropulsion*. Microsatellites represent the transition: at 100 kg propulsion systems can be shrunken down versions of traditional propulsion systems while by 10 kg they are likely to be very different systems. The general rule of thumb for microsatellites is that they have 1 W/kg of power available for propulsion. A total wet mass of the propulsion system itself is

typically 10-20% of the total mass of the satellite. In general the smaller the satellite the more integrated (sharing components with other subsystems) the propulsion system must be and the more MEMS fabrication will be used. All of the support hardware must also be shrunk. Issues arising from scaling propulsion systems to small dimensions produce a wide variety of concerns across the entire range of micropropulsion systems as shown in Table 18-18.

Table 18-18.Common Micropropulsion Concerns.

Scaling Issue	Concern	Affected Thrusters
Small Length Scale	High Heat Transfer	Chemical
	Passage Clogging	Chemical
	High Field Strengths	Electric
	Rarefied Flows	Chemical
	High Magnetic Fields	Electromagnetic
	Valve Leakage	All
	Voltage Limited	Electric
High Surface to Volume Ratio	Increase Heat Transfer	Chemical
	Increase Wall Losses	Electric
Short Residence Times	Limited Mixing Time	Bipropellant
	Frozen Flow Losses	Chemical
	Limited Vaporization Time	Chemical
Reynold's Number 10^2 - 10^4	High Viscous Losses	Chemical
	Limited Mixing	Chemical
Limited Materials/Manufacturing	Relative Surface Roughness	Chemical
	Compatibility Limitations	Chemical
	Nonuniform Properties	All

Propulsion systems from all classifications of full-scale propulsion have been successfully shrunk to the scale relevant for microsatellites. Additional new types of propulsion systems, such as solid propellant digital microthrusters, have also been developed, primarily for application at the smaller size scales (near 10 kg). Table 18-19 lists typical performance numbers for micropropulsion systems that have been demonstrated in the laboratory environment, but have typically not been flight qualified (TRL 3 - 6). Positions left blank lack sufficient published information to draw conclusions. With a sufficient developmental effort the majority of technologies listed in Table 18-19 could be flight ready in the next 10-20 years. Research is being conducted in the fields of nanopropulsion and picopropulsion, but in general the technologies are not sufficiently developed to warrant inclusion in the table.

Table 18-19. Representative Relatively Mature Micropropulsion Systems [Scharfe, 2009]

Thruster Type	Thrust [N]	I_{sp} [s]	Power [W]	Thruster Mass [kg]
Cold Gas	$5x10^{-4}$ – 3	40 – 80	---	0.01 – 1
Laser (Ignition)	$1x10^{-3}$ – $1x10^{-2}$	37 – 100	---	---
Monopropellant	$1x10^{-6}$ – 1.5	100 – 230	≤ 6	0.01 – 0.5

Decomposing Solid	---	230	---	---
Electrothermal	≤ 0.22	50 – 250	3 – 300	0.1 – 1
Laser (Ablation)	$1x10^{-6}$	100 – 300	2	---
Bipropellant	$1x10^{-6}$ – 45	100 – 320	≤ 6	0.01 – 0.5
Laser (Plasma)	$1x10^{-4}$ – $1x10^{-3}$	500 – 1000	2	≤ 1
Solar Thermal	$5.6x10^{-2}$ – 1	200 – 1100	---	≤ 10
Hollow Cathode	$1x10^{-6}$ – $1x10^{-2}$	50 – 1200	5 – 1000	---
Hall/Ion	$4x10^{-4}$ – $2x10^{-2}$	300 – 3700	14 – 300	≤ 1
Electromagnetic	$3x10^{-5}$ – $2x10^{-3}$	200 – 4000	≤ 10	0.06 – 0.5
FEEP/Colloid	$1x10^{-7}$ – $1.5x10^{-3}$	450 – 9000	1 – 100	0.1 – 1

18.7.3 Propulsion Systems for Very Large Satellites

In contrast with smallsats, however, some categories of satellites continue to increase in size. GEO communications satellites, for example, have steadily increased in size from approximately 35 kg with 28 Watts in 1963 (Syncom 2) to approximately 6910 kg (Terrestar-1) with up to 25 kW in total power in 2009 (Space Systems Loral 1300 series). It is assumed that there are no technical limitations to scaling chemical propulsion systems to the larger sizes relevant for this range of satellites. High performance electric propulsion systems at power levels of 100 – 200 kW, however, must be further developed. Several candidate technologies have already been demonstrated in the lab and are sufficiently well characterized to begin to make comparisons.

As mentioned in Sec. 18.6.3., a *magnetoplasmadynamic* (MPD) thruster is similar to an arcjet in physical geometry, but it accelerates the propellant using the Lorentz force as the ionized propellant passes through a high intensity arc. Two classifications of the MPD thruster exist depending on whether the magnetic field is self-generated (self field MPD) or externally applied (applied field MPD). Applied field MPDs are typically a more attractive option at lower power levels in 2009.

Hall thrusters for moderately sized spacecraft are a flight-qualified technology as described in Sec. 18.6.3. Traditional single channel Hall thrusters can become quite heavy at high-power levels, but it is conceivable that an array of small thrusters could be assembled to achieve power levels of 100s of kW at acceptable mass levels. The *NASA-457M* is chosen to represent the possibility of clustering existing systems [Manzella, 2002]. One way to overcome this limitation is to use a Hall thruster with multiple concentric channels. This allows the thruster channels to share the magnetic circuit and significantly reduce the thruster footprint. *Nested channel Hall (NHT)* thrusters are under development.

The *Variable Specific Impulse Magnetoplasma Rocket (VASIMR)* was designed as a high-power electric propulsion system so it has both high specific impulse (4000 – 5000 s) and high thrust (5 N). VASIMR has three different stages: a helicon radiofrequency (RF) section to ionize the plasma, a second RF section that uses ion cyclotron resonance frequency (ICRF) to further heat the plasma, and a superconducting electromagnetic nozzle as the final stage. Ground testing of a laboratory model (*VX-200*) has validated the expected performance levels of the device (η_t = 60 %, I_{sp} = 5000 s, P = 200 kW). A VASIMR device

(*VF-200*) will be tested on the international space station sometime around 2014 to demonstrate space-based performance.

A *plasmoid* is a coherent structure of plasma and its self-generated magnetic field. *Field reverse configuration* (FRC) is a particular method of generating a plasmoid where an axial bias field is rapidly reversed producing closed field lines that confine the plasmoid against its thermal pressure. The plasmoid can then be accelerated using various methods. The *ELF-375* thruster being developed at MSNW uses a rotating magnetic field acceleration scheme to accelerate the plasmoid [Slough, 2009]. Inductive techniques do not require electrodes and could theoretically have longer lifetimes. Table 18-20 shows a comparison of the performance of various high power electric propulsion devices, scaled to 200 kW to allow a direct comparison.

Table 18-20. Performance of High-Power Electric Propulsion at 200 kW [Brown, 2010]

	NASA-457M Cluster (4 thrusters)	**High I_{sp} NHT (2 channels)**	**Moscow Aviation Institute 200kW AF-MPD**	**VASIMR VX-200 (design goals)**	**ELF-375 (design goals)**
Input Power (kW)	200 (4x50)	200	123 – 186	200	200
Specific Impulse (s)	1800 – 3500	4000 – 5000	2760 - 4240	4000 – 5000	1500 – 5000
Thrust (N)	7.6 – 9.5	5.3 – 6.1	4.5	5	7 – 18
Mass Flow Rate (mg/s)	220 – 540 (Xe)	100 – 160 (Kr)	92 – 128 (Li)	100 – 125 (Ar)	140 – 1200 (Xe)
Efficiency	42% – 65%	60% – 65%	35 – 50%	48% – 60%	65% – 85%
Specific Mass (kg/kW) Thruster Thruster + PPU	 2.2 3.1	 0.5 1.4	 --- ---	 1.5 ---	 0.25 0.70
Major Dimensions (m)	1.1 by 1.1 0.15 length	0.69 diam. 0.10 length	--- ---	1.5 diam. 3.0 length	0.38 diam. 0.50 length

Several of the more developed technologies (clustered Hall thrusters, nested Hall thrusters, and VASIMR) could be flight ready in the next 10 years while MPD thrusters and the ELF thruster would likely take longer to be fully developed. The primary limitation for all of the technologies is the inability to test any of them on the ground for significant periods.

18.8 Examples

18.8.1 FireSat II

Continuing with the example of the Fire Sat II we know that the total ΔV required is 764 m/s. FireSat II is a 3-axis stabilized spacecraft. The total ΔV represents the needs for translational motion and for

unloading the reaction wheels. At this point, we don't know the split between them but we can still get a preliminary mass budget for the propulsion system.

In order to provide pure moments around an axis, without a resultant force, we need 2 thrusters. Thus, a total of 6 thrusters would be needed for stabilizing a spacecraft in 3 axes. In practice, 4 reaction wheels can provide pure rotations in all axes. The unloading of the wheels can be accomplished with 4 thrusters (or 8 to be fully redundant). However, when using 4 thrusters, you can have resultant forces in addition to a rotation about a given axis. For this example, we will assume we have 4 thrusters for unloading the wheels and 1 main thruster for primary propulsion.

The ΔV needed for Fire Sat II is within the range of monopropellants thrusters, but let's compare several options before we decide. From Sec. 14.7, we know the payload mass is 20 kg but we are carrying a 30% margin so the total payload mass is,

$M_{payload\_max} = 20 \text{ x } 1.3 = 26 \text{ kg}$

From Table 14.5-2, LEO with propulsion, we calculated in Sec. 14.7 that the payload is 31% of the dry mass, so

$M_{dry} = M_{payload\_max}/0.31 = 84 \text{ kg}$

Since we know the final mass (M_{dry}) we can use the rocket equation (18-19) to calculate how much propellant is required. However, we need to assume a value of I_{sp}. If we choose different types of thrusters for translational motion and for attitude control, then the propellant masses for each type of thruster need to be calculated separately. At this point, though, we don't know what the thrust requirements are for each class of thruster, so let's pick an "average" I_{sp} for the system. Considering monopropellants, (Table 18-5) the I_{sp} varies from about 200-235 s. For this example, let's choose an intermediate value of I_{sp} = 218 s. Substituting this into the rocket equation (18-19) we obtain the propellant mass needed,

$$M_p = M_f(e^{\Delta V / I_{sp} g_o} - 1) = 84(e^{764/(218 \times 9.81)} - 1) = 36.1kg$$

For the attitude control maneuvers, candidate thrusters could be the *MRE-1.0* or the *MRC-111,* which have the added advantage of being flight-proven. From Table 18-5 we see that the mass of these thrusters varies from 0.33 to 1 kg. For estimation purposes, let's assume a mass of 1 kg per thruster. For the primary propulsion thruster, a potential candidate could be the *Monarc-445* (1.6 kg) but we would need to have more information on the thrust levels required before choosing a thruster.

To size a bipropellant system (Table 18- 6), let's take an average I_{sp} of 291 s, taken from values for low thrust engines like *5lb Cb* (0.82-0.91 kg) and the *10N Bipropellant thruster* (0.35-0.65 kg). In that case, the rocket equation would give us M_p = 25.8 kg. That is a savings of 10.3 kg in propellants compared to the monopropellant system. We would need to compare the masses of the monopropellant and bipropellants thrusters to see if the savings in mass are enhanced or reduced. Looking at Figure 18- a bipropellant system is much more complicated (more components that can malfunction) and costly than

a monopropellant one. Therefore, we need to trade the price, availability (and the other -ilities described in Table 18-1) of the two systems to see if the added mass of the monopropellant is justified.

Assuming that after the different trades, a monopropellant system is chosen, the mass of the tank can be estimated by using Sec. 18.5.1. From the propellant mass calculated above and using the density of hydrazine at 293 K from Table 18-8, 1.01 g/cm^3, the volume of the propellant needed is,

$$V_{prop} = \frac{m_{prop}}{\rho_{prop}} = \frac{36.1kg}{1.01kg/L} = 35.7L$$

Let's take 20% margin on the volume (42.9 L), then From Figs. 18-9 and 10 respectively, the mass of the tank can range from 4.1 to 5.5 kg for a PMD and a diaphragm tank respectively. As a baseline, let's take the diaphragm tank since it represents a worst-case scenario for the weight and it can handle a large array of accelerations. The next step is to decide whether this system will be blow-down or pressurized. Since we have some commercial off-the-shelf thrusters that could potentially meet our needs, we would contact the manufacturer and get all the details from them. However, for this example, we will assume that simplicity is more important than performance, so we can baseline a blow-down system.

The last thing to estimate is the mass for the feed system. A good estimate would involve creating a schematic like the one shown in Fig. 18-8b and determining the quantity and type of required valves, filters, transducers, etc., along with the length, diameter and material of the tubing used. Without that information, as a rule of thumb for liquid propulsion systems, the mass of the tank and plumbing is about 10% of the total mass of the propulsion system and it can be higher for smaller thrusters. Assuming 15%, to be conservative we obtain for the mass of the feed system,

$M_{tank} + M_{feed} = 0.1 \text{ x } (M_{tank} + M_{feed} + M_{propellant} + M_{thruster})$

$M_{feed} = 0.176 \text{ x } (M_{propellant} + M_{thruster}) - M_{tank} = 0.176 \text{ x } (36.1 + [4 \text{ x } 1 + 1.6]) - 5.5 = 1.9 \text{ kg.}$

The total mass estimate is 49.1 kg. The preliminary mass budget for the propulsion system for Fire Sat II is shown in Table 18.21.

18.8.2 Supplemental Communications System

Marc Young, ***Air Force Research Laboratory, Edwards, California***

The initial design for the SCS satellite requires thrusters for both primary propulsion and for unloading of the reaction wheels for the 3-axis stabilized spacecraft. These requirements commonly lead to a propulsion configuration involving four total thrusters (or eight total thrusters if full redundancy is required). All of the thrusters will be aimed approximately 15 degrees off the primary axis (z-axis) in the +x, -x, +y, -y directions. All four will fire simultaneously for a delta v maneuver while less than four thrusters fire together when a rotation required. A single common propellant and tank will be used in the system. The total mission ΔV (including margin and ullage) has been estimated to be 90 m/s which is relatively low for satellite systems. These early requirements already indicate that thruster simplicity will be an important consideration along with thruster performance (specific impulse). Hydrazine

monopropellant thrusters are commonly used for the required roles, but cold gas thrusters should also be evaluated because of their inherent simplicity. The two thruster systems can be evaluated based on their ability to provide the required total mission ΔV without consuming too much of the mass budget (total spacecraft mass of 200 kg).

The first step in choosing the propulsion system is to evaluate the amount of required propellant based on the rocket equation (Eq. 18-19). Cold gas thrusters with low leak rate propellants typically have I_{sp} of 45 to 73 s (Table 18-4). For the SCS mission, cold gas thrusters would require 23 – 37 kg of propellant based on the above I_{sp} range and assuming ΔV =90 m/s. Hydrazine monopropellant thrusters typically have specific impulses between 215 and 235 s (Table 18-5). Applying the rocket equation again (Eq. 18-19), for the above I_{sp} values, the SCS mission hydrazine thrusters would require between 7.7 and 9.0 kg of propellant. It is unlikely that the projected propellant mass savings for the hydrazine system (roughly 20 kg) could be overcome by the dry mass savings of the cold gas system. With the significant flight heritage of hydrazine monopropellant thrusters they are a good first choice for the SCS system.

Sizing of the propulsion system can continue by choosing appropriately sized thrusters with flight heritage to use as examples. The single thruster module of the MRE-1.0 system can meet the thrust requirement of 4.5N and has a mass of 0.5 kg and an I_{sp} of 218 s (shown on Table 18-5). The rocket equation (Eq. 18-19) indicates that a mission with a total ΔV of 90 m/s would require 8.2 kg of propellant at a specific impulse of 218 s. The SCS system requires four single thruster modules yielding a total thruster mass of 2.0 kg. To finish the mass estimates we must estimate the mass for the propellant tank and feed system. A simple diaphragm blow-down tank is chosen for this example problem because of its simplicity and the ability of monopropellant thrusters to operate over a wide range in pressures. According to Table 18-8, hydrazine has a density of 0.982 g/cm^3 at an assumed high temperature of 323 K. This yields a required propellant volume of 8.35 liters. Adding the recommended volume margin of 20% yields a recommended tank volume of 10.0 liters. The curve fit from Fig. 18-10 then yields a propellant tank mass of 1.6 kg. The general rule of thumb for liquid systems is that tank and feed system represent 10% of the total propulsion system mass (propellant + tank(s) + thruster + feed system). In the SCS system, as is common with small-scale satellites, the tank and feed system could represent a higher fraction. Assuming that the tank and feed system accounts for 20% of the total mass of the propulsion system, that is,

$$M_{tank} + M_{feed} = 0.2 \times (M_{tank} + M_{feed} + M_{propellant} + M_{thruster})$$

then, the tank (1.6 kg) and feed system (1.0 kg) would have a total mass of 2.6 kg yielding a total propulsion system mass of approximately 12.8 kg. The breakdown of the propulsion system mass budget is given in Table 18-21. The next step in the design process would be to create a system design including all required components which would yield a schematic similar to the one in Fig. 18-8b.

Table 18-21. Preliminary Mass Budget for Fire Sat II and SCS.

	Fire Sat II	SCS

Propellant (kg)	36.1	8.2
Thrusters (kg)	5.6	2.0
Tank (kg)	5.5	1.6
Feed System (kg)	1.9	1.0
Total Mass of Propulsion System (kg)	49.1	12.8

REFERENCES

1. Aerojet Redmond. 2003. *MR-502A Improved Electrothermal Hydrazine Thruster (IMPEHT) Data Sheet*. Redmond, WA: Aerojet Redmond. April.
2. Aerojet Redmond. 2003. *MR-509 Low Power Arcjet System Data Sheet.* Redmond, WA: Aerojet Redmond. April.
3. Aerojet Redmond. 2003. *MR-510 Arcjet Thruster and Cable Assembly Data Sheet*. Redmond, WA: Aerojet Redmond. April.
4. Aerojet Redmond. 2003. *BPT-4000 Hall Effect Thruster Data Sheet*. Redmond, WA: Aerojet Redmond, April.
5. AIAA. 1999. "AIAA Standard for Space Systems – Metallic Pressure Vessels, Pressurized Structures, and Pressure Components," S-080-1998e.
6. AIAA. 2006. "AIAA Standard for Space Systems – Composite Overwrapped Pressure Vessels (COPVs)," S-081A-2006e. Revised.
7. Air Force Space Command. 2004. "Range safety user requirements manual – volume 2 flight safety requirements," Manual 91-710 Vol. 2 (AFSPCMAN 91-710 V2).
8. Astrium EADS. 2010. *cs.astrium.eads.net*. April.
9. Astrium EADS. 2010. : http://cs.astrium.eads.net/sp/SpacecraftPropulsion/MonopropellantThrusters.html. October.
10. Astrium EADS. 2010. http://cs.astrium.eads.net/sp/LauncherPropulsion/Brochures/aestus.pdf. October.
11. Astrium EADS. 2010. http://cs.astrium.eads.net/sp/SpacecraftPropulsion/Bipropellant_Thrusters/400N_Bipropellant_Apogee_Engine_S400.html. October.
12. Astrium EADS. 2010. http://cs.astrium.eads.net/sp/Brochures/PDF/10N%20Bipropellant%20Thruster.pdf. October.

13. Bae, Y. 2007. "Photonic Laser Propulsion: Photon Propulsion Using and Active Resonant Optical Cavity," paper no. AIAA-2007-6131 presented at the AIAA Space 2007 Conference. Long Beach, CA, September 18-20.

14. Bae, Y. 2008. "Photonic Laser Propulsion: Proof-of-Concept Demonstration," *Journal of Spacecraft and Rockets*. 45:153-155.

15. Balaam, P. and M. M. Micci. 1995. "Investigation of Stabilized Resonant Cavity Microwave Plasmas for Propulsion." *Journal of Propulsion and Power*. Vol. 11, No. 5, September-October 1995, pp. 1021.

16. Benson, S., L. A. Arrington, W. A., Hoskins, N. J. Meckel.1999. "Development of a PPT for the EO-1 Spacecraft," paper no. AIAA-1999-2276 presented at the 35th Joint Propulsion Conference and Exhibit. Los Angeles, CA, June 20-24.

17. Bergonz, F. 1982. *Manned maneuvering unit*, NASA Johnson Space Center Satellite Serv. Workshop, Vol. 1 p 32-43 (SEE N83-11175 02-16).

18. Bolonkin, A. 2006. *Non-Rocket Space Launch and Flight*. Oxford, UK: Elsevier.

19. Brown, C. D. 1996. *Spacecraft Propulsion,* AIAA Education Series.

20. Brown, C.D. 2002. *Elements of Spacecraft Design*. AIAA Education Series.

21. Brown, D. L. 2010. Personal Communication.

22. Burton, R. L. and P. J. Turchi. 1998. "Pulsed Plasma Thruster." *Journal of Propulsion and Power.* Vol. 14, No. 5, September-October, pp. 716-735.

23. Busek Company. 2007. *Low Power Hall Effect Thruster Systems Data Sheet, 2nd ed*. Natik, MA:Busket Company.

24. Busek Company. 20087. *High Power Hall Effect Thruster Systems Data Sheet.* Natik, MA:Busek Company.

25. Busek Company. 2007. *Micro Pulsed Plasma Thruster Data Sheet*. Natik, MA:Busek Company.

26. Bzibziak, R. 2000. "Update of Cold Gas Propulsion at Moog," paper no. AIAA 2000-3718 presented at the 36th Joint Propulsion Conference and Exhibit. Huntsville, AL, July 17-19.

27. Bzibziak, R. 2010. Private Communication.

28. Cassidy, R. J., W. A. Hoskinsand C. E. Vaughn. 2002. "Development and Flight Qualification of a 26-Kilowatt Arcjet Propulsion Subsystem." *Journal of Propulsion and Power*. Vol. 18, No. 4, July-August, pp. 740-748.

29. Chiaverini, M. J., K. K. Kuo, eds. 2007. *Fundamentals of Hybrid Rocket Combustion and Propulsion*. Progress in Astronautics and Aeronautics, Vol. 218.

30. Choueriri, E. Y. 2004. "A Critical History of Electric Propulsion: The First 50 Years (1906-1956)." *Journal of Propulsion and Power*. Vol. 20, No. 2, March-April.

31. Choueriri, E. Y. and K. A. Polzin. 2006. "Faraday Acceleration with Radio-Frequency Assisted Discharge." *Journal of Propulsion and Power.* Vol. 22, No. 3, May-June, pp. 611-619.

32. Clark, J. D. 1972. *Ignition! An Informal History of Liquid Rocket Propellants*. New Brunswick, NJ: Rutgers University Press.

33. Cole, J., I. Silvera, J. Foote. 2008. "Conceptual Launch Vehicles Using Metallic Hydrogen Propellant," in *Proceedings of the Space Technology and Applications International Forum-STAIF 2008*, ed. M.S. El-Genk, Melville, NY: AIP, Vol. 969, pp. 977-984.

34. Dawnson, M., G. Brewster, C. Conrad., M. Kilwine, B. Chenevert, O. Morgan. 2007. "Monopropellant Hydrazine 700 lbf Throttling Terminal Descent Engine for Mars Science Laboratory," paper no. AIAA 2007-5481 presented at the 43rd AIAA/ASME/SAE/ASEE Joint Propulsion Conference and Exhibit. Cincinnati, OH, July 8-11.

35. Dornheim, M. A. 2003. "Ideal hybrid fuel is … wax?" *Aviation Week & Space Technology*. February 3, p.50.

36. Dornheim, M. A. 2003. "Burt Rutan's quest for space." *Aviation Week & Space Technology*. April 21, p.64.

37. Dressler, R., Y. Chu, D. J. Levandier. 2000. "Propellant Alternatives for Ion and Hall EffectThrusters," paper no. AIAA-2000-0602 presented at the 38th Aerospace Sciences Meeting and Exhibit. Reno, NV. January 10-13.

38. Drenning, C. K., R. J. Phillips, R.V. Loustau, F.L. Falconer. 1978. "Design and Fabrication of Space Shuttle Reaction Control Thruster Insulated Scarf Nozzles," paper no. AIAA 1978-1006 presented at the 14th AIAA and SAE Joint Propulsion Conference. Las Vegas, NV, July 25-27.

39. Dyer, J., E. Doran, Z. Dunn, K. Lohner, C. Bayart, A. Sadhwani, G. Zilliac, B. Cantwell, A. Karabevoglu. 2007. "Design and Development of a 100km Nitrous Oxide/Paraffin Hybrid Rocket Vehicle," paper no. AIAA 2007-5362 presented at the 43rd AIAA and SAE Joint Propulsion Conference. Cincinnati, OH, July 8-11.

40. Evans, B., E. Boyer, K. Kuo, G. Risha, M. Chiaverini. 2009. "Hybrid Rocket Investigations at Penn State University's High Pressure Combustion Laboratory: Overview and Recent Results," paper no. AIAA-2009-5349 presented at the 45th AIAA/ASME/SAE/ASEE Joint Propulsion Conference. Denver, CO, August 2-5.

41. Ferguson, H. and J. S. Sovey, J. S. 1967. *Performance Tests of a 1/2-Millipound (2.2 mN) Ammonia Resistojet Thruster System.* Tech. rep., NASA Lewis Research Center.

42. Frei T. E., T.L. Fischer, J. M. Weiss. 2001. "Mars Polar Lander Thruster Cold Start Validation Testing," paper no. AIAA-2001-3261 presented at the 37th AIAA/ASME/SAE/ASEE Joint Propulsion Conference. Salt Lake City, UT, July 8-11.

43. General Electric Space Division. 1978. *Landsat 3 Reference Manual*, Philadelphia, PA.

44. Gesto, F., B. Blackwell, C. Charles, R. Boswell. 2006. "Ion Detachment in the Helicon Double-Layer Thruster Exhaust Beam." *Journal of Propulsion and Power*. Vol. 22, No. 1, January-February, pp. 24-30.

45. Goddard, E. C. and G. E. Penray (editors). 1970. *The Papers of Robert H. Goddard*. McGraw-Hill Book Company.

46. Goebel, D. M. and I. Katz. 2008. *Fundamentals of Electric Propulsion: Ion and Hall Thrusters*. Vol. 1, JPL Space Science and Technology Series, John Wiley and Sons, Inc., New York, 1st ed.

47. Henshall, P., P. Palmer. 2006. "Solar Thermal Propulsion Augmented with Fiber Optics: Technology Development," paper no. AIAA-2006-4874 presented at the 42nd AIAA/ASME/SAE/ASEE Joint Propulsion Conference. Sacramento, CA, July 9-12.

48. Hill, P., C. Peterson. 1992. *Mechanics and Thermodynamics of Propulsion*, 2nd Edition. Addison-Wesley Publishing Company.

49. Hill, C. S. 1980. "SSRCS First Flight Certification Testing," paper no. AIAA 1980-1130 presented at the 16th SAE and ASME Joint Propulsion Conference. Hartford, CT, June 30-July 2.

50. Hofer, R. R. and A. D. Gallimore. 2006. "High Specific Impulse Hall Thrusters, Part 2: Efficiency Analysis." *Journal of Propulsion and Power*. Vol. 22, No. 4, July-August, pp. 732-740.

51. Holmberg N. A., R.P. Faust, H.M. Holt. 1980. *Viking '75 Spacecraft Design and Test Summary*, NASA Reference Publication 1027.

52. Hruby, V., J. Kolencik, K. D. Annen, R. C. Brown. 1997. "Methane Arcjet Experiments," paper no. AIAA-1997-2427 presented at the 28th AIAA Plasma Dynamics and Lasers Conference. Atlanta, GA, June 23-25.

53. Humble, R. W., G. N. Henry, W. J. Larson. 1995. *Space Propulsion Analysis and Design*. Space Technology Series. 1st Edition, New York, NY: McGraw-Hill.

54. Huzel, D. K., D. H. Huang. 1992. *Modern Engineering for Design of Liquid-Propellant Rocket Engines,* AIAA.

55. Isakowitz S. J., J. B. Hopkins, J. P. Hopkins Jr. 2004. *International Reference Guide to Space Launch Systems*, 4th edition. AIAA.

56. Ito, T., N. Gascon, S. Crawford, M. A. Cappelli. 2007. "Experimental Characterization of a Micro-Hall Thruster." *Journal of Propulsion and Power*. Vol. 23, No. 5, September-October, pp. 1069-1074.

57. Jackman C.H., D.B. Considine, E. L. Fleming. 1996. "Space shuttle's impact on the stratosphere: an update". *J of Geophysical Research.* Vol. 101, No. D7, pp 12,523-12,529.

58. Jacobson, D. and D. Manzella. 2003. "50 kW Class Krypton Hall Thruster Performance," paper no. AIAA-2003-4550 presented at the 39th Joint Propulsion Conference and Exhibit. Huntsville, AL, July 20-23.

59. Jahn, R., 1968. *Physics of Electric Propulsion*. McGraw-Hill.

60. Joslyn, T. B., A.K. Ketsdever. 2010. "Constant Momentum Exchange between Microspacecraft Using Liquid Droplet Thrusters," paper no. AIAA-2010-6966 presented at the 46th AIAA/ASME/SAE/ASEE Joint Propulsion Conference and Exhibit. Nashville, TN, July 25-28.

61. Kare, J.T. 2002. "Near-Term Laser Launch Capability: The Heat Exchanger Thruster," in *Proceedings of the First International Symposium on Beamed Energy Propulsion*, ed. A.V. Pakhomov, AIP Conference Proceedings 664, Melville, NY, pp. 442-453.

62. Ketsdever, A. 2000. "System Considerations and Design Options for Microspacecraft Propulsion Systems", *Micropropulsion for small spacecraft*. Progress in Astronautics and Aeronautics, Vol. 187, edited by M. Micci and A. Ketsdever, AIAA Reston, VA, Chapter 4.

63. Ketsdever, A. D., M. P. Young, J. B. Mossman, A. P Pancotti. 2010. "Overview of Advanced Concepts for Space Access." *Journal of Spacecraft and Rockets*. 47:238-250.

64. Kodys, A. D., and E. Y. Choueiri. 2005. "A Critical Review of the State-of-the-Art in the Performance of Applied-field Magnetoplasmadynamic Thrusters," paper no. AIAA-2005-4247 presented at the 41st AIAA/ASME/SAE/ASEE Joint Propulsion Conference. Tucson, AZ, July 11-13.

65. Legge, R. S., P. Lozano, M. Martinez-Sanchez, M. 2007. “Fabrication and Characterization of Porous Metal Emitters for Electrospray Thrusters," paper no. IEPC-2007-145 presented at the 43rd Joint Propulsion Conference and Exhibit. Florence, Italy, September 17-20.

66. Lichon, P. G. and J. M. Sankovic. 1996. “Development and Demonstration of a 600-Second Mission-Average Isp Arcjet." *Journal of Propulsion and Power*. Vol. 12, No. 6, November-December, pp. 1018-1025.

67. Linnell, J. A. and A. D. Gallimore. 2006. “Efficiency Analysis of a Hall Thruster Operating with Krypton and Xenon." *Journal of Propulsion and Power*. Vol. 22, No. 6, November-December, pp. 1402-1418.

68. Lockheed Martin Corp. 2005. (http://www.lockheedmartin.com/news/press_releases/2005/LOCKHEEDMARTINSUCCESSFULLYTESTFIRES.html). November.

69. Loeb, H. W., D. Feili, B. K. Meyer.2004. “Development of RIT Microthrusters”, paper no. No. IAC-04-S.4.04 presented at the 55th International Astronautical Congress, American Institute of Aeronauticsand Astronautics, Vancouver, October.

70. Manzella, D., R. Jankovsky, R. Hofer. 2002. "Laboratory Model 50 kW Hall Thruster," paper no. AIAA-2002-3676 presented at the 38th AIAA/ASME/SAE/ASEE Joint Propulsion Conference, Indianapolis, IN, July 7-10.

71. Martin, A. and R. Eskridge. 2005. “Electrical Coupling Efficiency of Inductive Plasma Accelerators." *Journal of Physics D: Applied Physics*. Vol. 38, November, pp. 4168-4179.

72. McRight, P., C. Popp, C. Pierce, A. Turpin, W. Urbanchock. 2005. “Confidence Testing of Shell-405 Catalysts in a Monopropellant Hydrazine Thruster,” paper no. AIAA-2005-3952 presented at the 41st AIAA/ASME/SAE/ASEE Joint Propulsion Conference. Tucson, AZ, July 10-13.

73. Messerschimd, E. W., D. M. Zube, K.Meinzer, H. L. Kurtz. 1996. “Arcjet Developmentfor Amateur Radio Satellite." *Journal of Spacecraft and Rockets*. Vol. 33, No. 1, January-February, pp. 86-91.

74. Micci, M. M. and Ketsdever, A. D., Micropropulsion for Small Spacecraft, Progress in Astronautics and Astronautics, V-187, American Institute of Aeronautics and Astronautics, 2000.

75. Mikellides, P. G. and C. Neilly. 2007. “Modeling and Performance Analysis of the Pulsed Inductive Thruster." *Journal of Propulsion and Power*. Vol. 23, No. 1, January-February, pp. 51-58

76. Moog. 2010. http://www.moog.com/products/propulsion-controls/spacecraft/components/cold-gas-thrusters/solenoid-actuated. November.

77. Morgan, J. A. 1997. "A Brief History of Cannon Launch," paper no. AIAA-1997-3138 presented at the 33rd AIAA/ASME/SAE/ASEE Joint Propulsion Conference. Seattle, WA, July 6-9.

78. Morrisey, D. C. 1992. “Historical perspective - Viking Mars Lander propulsion.“ *Journal of Propulsion and Power*. Vol. 8, No. 2, pp. 320-331.

79. Morring, Jr., F. 2003. “Test puts Hybrid Rockets back on the Table.” *Aviation Week & Space Technology*. February 3, p.50.

80. Myrabo, L., D. Messitt, F. Mead. 1998. "Ground and Flight Tests of a Laser-Boosted Vehicle," paper no. AIAA-1998-1001 presented at the 36th Aerospace Sciences Meeting and Exhibit. Reno, NV, Jan. 12-15.

81. National Research Council. 1998. *Assessment of Exposure-Response Functions for Rocket-Emission Toxicants, Subcommittee on Rocket-Emission Toxicants*. Committee on Toxicology, Board on Environmental Studies and Toxicology, Commission on Life Sciences, National Academy Press, Washington, D.C.

82. Norris, G. 2009. "Virgin Galactic's SpaceShip Two Revealed in Desert Rollout." *Aviation Week & Space Technology*. Dec. 14, p.37

83. Northrop Grumman Space Technology; Propulsion Systems. 2010. http://www.as.northropgrumman.com/products/monoprpellant_thrust/index.html. November.

84. Northrop Grumman Space Technology; Propulsion Systems. 2010. http://www.as.northropgrumman.com/products/bipropellant_engines/index.html. November.

85. Oda, Y., K. Komurasaki, K.Takahashi,A. Kasugai, K. Sakamoto. 2006. "Plasma Generation Using High-Power Millimeter-Wave Beam and Its Application for Thrust Generation." *J. Appl. Phys*. 100: 113307.

86. Parkin, K.L. 2006. "The Microwave Thermal Thruster and Its Application to the Launch Problem," PhD Thesis, California Institute of Technology.

87. Peterson, P., D. Jacobson, D. Manzella, J. John, J. 2005. "The Performance and Wear Characterization of a High-Power High-Isp NASA Hall Thruster," paper no. AIAA-2005-4243 presented at the 41st Joint Propulsion Conference and Exhibit. Tucson, AZ, July 10-13.

88. Phipps, C., J. Luke, T. Lippert, M. Hauer, A. Wokum. 2004. "Micropropulsion Using a Laser Ablation Jet." *Journal of Propulsion and Power*. Vol. 20, No. 6, November-December, pp. 1000-1011.

89. Phipps, C. R. 2006. *Laser Ablation and Its Applications*. Springer-Verlag, New York.

90. Pidgeon, D. J., R. L. Corey, B. Sauer, M. L. Day. 2006. "Two Years On-Orbit Performance of SPT-100 Electric Propulsion," paper no. AIAA-2006-5353 presented at the 24th International Communications Satellite Systems Conference. San Diego, CA, June 11-14.

91. Poehlmann, F. and M. A. Cappelli. 2007. "The Deflagration-Detonation Transition in Gas-FedPulsed Plasma Accelerators," paper no. AIAA-2007-5263 presented at the 43rd Joint Propulsion Conference and Exhibit. Cincinnati, OH, July 8-11.

92. "Projects, Organizations, and Missions." Online. Available http://www.ugcs.caltech.edu/~diedrich/solarsails/links/, July 14, 2002.

93. QinetiQ. 2004.*GOCE T5 Based Electric Propulsion System Data Sheet*. United Kingdom:QinetiQ.

94. Schapell, D. T., E. Scarduffa, P. Smith, N. Solway. 2005. "Advances in Marotta Electric and Small Satellite Propulsion Fluid Control Activities," paper no. AIAA-2005-4055 presented at the 41st Joint Propulsion Conference and Exhibit. Tucson, AZ, July 10-13.

95. Semenkin, A., A. Kochergin, A. Rusakov, V.Bulaev, J.Yuen, J. Shoji, C.Garner, D. Mazella. 1999."Development Program and Preliminary Results of the TAL-110 Thruster," paper no. AIAA-1999-2279 presented at the 35th Joint Propulsion Conference and Exhibit. Los Angeles, CA, June 20-24.

96. Simmons, F.S. 2000. *Rocket Exhaust Plume Phenomenology*. The Aerospace Press.

97. Slough, J., D. E. Kirtley,T. Weber. 2009. "Pulsed Plasmoid Propulsion: The ELF Thruster," paper no. IEPC-2009-265, presented at the International Electric Propulsion Conference. Ann Arbor, MI, Sept. 20-24.

98. Smith, P. 2006. "Resistojet Thruster Design and Development Programme," paper no. AIAA-2006-5210 presented at the 42nd Joint Propulsion Conference and Exhibit. Sacramento, CA, July 9-11.

99. Smith, K. L., M.S. Alexander, M. D. Paine, J. P. W. Stark. 2009. "Scaling of a Colloid Thruster System for MicroNewton to MilliNewton Thrust Levels," paper no. IEPC-2009-112 presented at the 30thInternational Electric Propulsion Conference. Ann Arbor, MI, September 20-24.

100. Stechman R. C. 1985. "Modification of the Space Shuttle Primary Thruster (870 lbf) for Apogee and Perigee Kick Stages," paper no. AIAA 1985-1222 presented at the 21st SAE, ASME and ASEE Joint Propulsion Conference. Monterey, CA, July 8-10.

101. Stechman R. C. 1990. "Development History of the 25 lbf (110 Newton) Space Shuttle Vernier Thruster," paper no. AIAA 1990-1837 presented at the 26th SAE, ASME and ASEE Joint Propulsion Conference. Orlando, FL, July 16-18.

102. Stechman C. R., P. Woll, R. Fuller, A. Colette. 2000. "A High Performance Liquid Rocket Engine for Satellite Main Propulsion," paper AIAA 2000-3161 presented at the 36th AIAA/ASME/SAE/ASEE Joint Propulsion Conference and Exhibit. Huntsville, AL, July 16-19.

103. Stwalley, W. 1991. "Survey of Potential Novel High Energy Content Metastable Materials," in *Proceedings of the High Energy Density Matter (HEDM) Conference*. Albuquerque, NM, February 24-27, (Phillips Lab PL-CP-91-3003, p. 3).

104. Sullivan, D. J., J. F. Kline, R. B. Miles, S. H. Zaidi. 2004. "A 300 W Microwave Thruster Design and Performance Testing," paper no. AIAA-2004-4122 presented at the 40th Joint Propulsion Conference and Exhibit. Fort Lauderdale, FL, July 11-14.

105. Sund, D. C., C.S. Hill.1979. "Reaction Control System Thrusters for Space Shuttle Orbiter," paper no. AIAA 1979-1144 presented at the 15th SAE and ASME Joint Propulsion Conference. Las Vegas, NV June 18-20.

106. Surrey Satellite Technologies, Ltd. 2007.*SSTL Low Power Resistojet Data Sheet SSTL-9029-02*. United Kingdom: Surrey Satellite Technologies. August.

107. Sutton, G. P. and O. Biblarz. 2010. *Rocket Propulsion Elements*, John Wiley and Sons, Inc., 7th ed.

108. Sweetman B., (editor). 2006. *Jane's Space Directory, 2006-2007*. Jane's Information Group.

109. Sweetman, B., (editor). 2008. *Jane's Space Systems and Industry 2008-2009*. Jane's Information Group.

110. Swink, D. G., O. M. Morgan, J. C. Robinson. 1999. *"Design and analysis of a low-cost reaction control system for GPS llF,"* paper no. AIAA 1999-2469, presented at the 35th Joint Propulsion Conference and Exhibit. Los Angeles, CA, June 20-24.

111. Tajmar, M. 2003. *Advanced Space Propulsion Systems.* Austria, Springer-Verlag.

112. Takao, Y., H. Kataharada, T.Miyamoto, H.Masui,N.Yamamoto, H. Nakashima. 2006. "Performance Test of Micro Ion Thruster Using Microwave Discharge." *Vacuum.* Vol. 80, No. 11-12, September, pp. 1239-1243.

113. Thompson, D. 2001. “Amine Azides used as monopropellants”, US Patent 6,299,654 B1.

114. Thompson P. A. 1972. *Compressible Fluid Dynamics*, McGraw-Hill, Inc.

115. Tikhonov, V. B., S. A. Semenkin, J. R. Brophy, J. E. Polk. 1997. “Performance of 130kWMPD Thruster with an External Magnetic Field and Li as Propellant," paper no. IEPC-1997-117 presented at the 25th International Electric Propulsion Conference. Cleveland, OH, August 24-28.

116. Tishkoff, J. M., and M. R. Berman. 2002. "Air Force Basic Research in Propellants and Combustion," paper no. AIAA-2002-0901 presented at the 40th AIAA Aerospace Sciences Meeting. Reno, NV, Jan. 14-17.

117. Toki, K., Y. Shimizu, K. Kurki. 2000. “On-Orbit Demonstration of a Pulsed Self-Field Magnetoplasmadynamic Thruster System." *Journal of Propulsion and Power*. Vol. 16, No. 5, September-October.

118. Tsander, F. A., From A Scientific Heritage, NASA TTF-541, 1967 (quoting from author 1924 report).

119. Tsiolkovskii, K. E., *Extension of Man Into Outer Space*, 1921.

120. Tsohas, J., B. Appel, A. Rettenmaier, M. Walker, S. Heister. 2009. “Development and Launch of the Purdue Hybrid Rocket Technology Demonstrator,” paper no. AIAA-2009-4842 presented at the 45th AIAA/ASME/SAE/ASEE Joint Propulsion Conference, Denver, CO, Aug. 2-5.

121. Turner, M. J. L., 2009. *Rocket and Spacecraft Propulsion*, 3rd Edition, Springer.

122. Tverdokhlebov, S. O., A. V. Semenkin, J. E. Polk. 2002. “Bismuth Propellant Option for Very High Power TAL Thruster," paper no. AIAA-2002-0348 presented at the 40th AIAA Aerospace Sciences Meeting and Exhibit. Reno, NV, January 14-17.

123. Vial, V. and O. Duchemin. 2009. “Optimization of the PPS Rx000-Technological Demonstrator for High ISP Operation," paper no. AIAA-2009-5283 presented at the 45th Joint Propulsion Conference and Exhibit. Denver, CO, Aug. 2-5.

124. Wangsness, R. K. 1986. *Electromagnetic Fields*. John Wiley and Sons, Inc., New York, 2nd ed.

125. Warner, N. Z. and M. Martinez-Sanchez. 2006. “Design and Preliminary Testing of a Miniaturized TAL Hall Thruster," paper no. AIAA-2006-4994 presented at the 42nd Joint Propulsion Conference and Exhibit. Sacramento, CA, July 9-12.

126. Wertz, J. R. and W. Larson (editors). 1999. *Space Analysis and Mission Design*. Microcosm Press and Springer. Hawthorne, 3rd ed.

127. Wu, P. -K., P. Woll, C. Stechman, B. McLemore, J. Neiderman, C. Crone. 2001. “Qualification Testing of a 2nd Generation High Performance Apogee Thruster,” paper no. AIAA 2001-3253 presented at the 37th AIAA/ASME/SAE/ASEE Joint Propulsion Conference and Exhibit. Salt Lake City, UT, July 8-11.

128. Zeimer, J. K. 2009. “Performance of Electrospray Thrusters," Paper No. IEPC-2009-242 presented at the 30th International Electric Propulsion Conference. Ann Arbor, MI, September.

Bibliography for the Solar Sail Section

1. Tsiolkovskii, K. E., Extension of Man into Outer Space, 1921.
2. Tsander, F. A., "On Using the Force of Light Pressure for Flights into Interplanetary Space," pp. 361 – 381, The Problem of Flying Using Rocket Devices: Interplanetary Flights [Russian], 2nd Edition, Moscow, Oborongiz, 1961.
3. Tsander, F. A., From a Scientific Heritage, NASA TTF-541, 1967 (quoting from author 1924 report).
4. Wiley, C., (pseudonym: Sanders, R.), "Clipper Ships of Space", Astounding Science Fiction, p. 135, May 1951.
5. Garwin, R. L., "Solar Sailing – A Practical Method of Propulsion within the Solar System," Jet Propulsion, Vol. 28, March 1958, pp. 188 – 190.
6. Wright, J. L., Solar Sailing: Evaluation of Concept and Potential, Battelle Memorial Institute Report, No. BMI-NLVP-TM-74-3, Nov. 1974.
7. Wright, J. L. and Warmke, J., "Solar Sailing Mission Applications," AIAA/AAS Astrodynamics Conference, August 1976, Paper No. 76-808.
8. Friedman, L., et al, "Solar Sailing – The Concept Made Realistic," AIAA 16th Aerospace Sciences Meeting, Jan. 1978.
9. "Solar Sail Unfurled," Bulletin – Quarterly Report of the Solar Sail Project, Vol. II, No. 3, July – Sept. 1981.
10. Koryo, M., Prado, J., Staehle, R., "Report on SSU, U3P, and Foundation Activities for the Earth-Moon Race," 42nd Congress of the International Astronautical Federation, October 5 – 11, 1991.
11. "Projects, Organizations, and Missions." Online. Available **http://www.ugcs.caltech.edu/~diedrich/solarsails/links/**, July 14, 2002.
12. "Cosmos 1: The First Solar Sail." **http://www.planetary.org/solarsail/who_where_when.htm**, July 5, 2002.
13. "Other Solar Sail Developments." **http://www.planetary.org/solarsail/other-sails.htm**, July 5, 2002.
14. "General Astronautics Services and Products." Online. Available **http://www.spacecityone.com/genastro/serviceproduct.htm**, July 5, 2002.
15. Blomquist, R., "Solar Blade Nanosatellite Development: Heliogyro Deployment, Dynamics, and Control," Proceedings of the 13th Annual AIAA/USU Conference on Small Satellites, August 1999.
16. Forward, R. L., "Statite: A Spacecraft That Does Not Orbit," J. Spacecraft 28, #5, 606-611 (Sept-Oct 1991).
17. Forward, R. L., "The Statite: A Non-Orbiting Spacecraft," AIAA 89-2546, AIAA/ASME/SAE/ASEE 25th Joint Propulsion Conference, Monterey, CA, July 10-12, 1989.
18. U.S. Patent 5,183,225 "Statite: Spacecraft That Utilizes Light Pressure and Method of Use," R.L. Forward, filed 9 January 1989, issued 2 February 1993, 4 claims (Forward Unlimited FUN-89/002).
19. Forward, R. L., "Light-Levitated Geostationary Cylindrical Orbits Using Perforated Light Sails," Technical Note, The Journal of the Astronautical Sciences, Vol. 32, No. 2, April – June 1984, pp. 221 – 226.
20. Forward, R. L., "Light-Levitated Geostationary Cylindrical Orbits: Correction and Expansion," The Journal of the Astronautical Sciences, Vol. 38, No. 3, July-September 1990, pp. 335-353.
21. "Solar Sail Technology Development 15-Year Roadmap." Online. Available **http://solarsail.jpl.nasa.gov/roadmap/images/roadmap-15-year2.gif**, July 14, 2002.
22. Friedman, L. D., *Starsailing: Solar Sails and Interstellar Travel*, John Wiley & Sons, 1988.
23. Bass, M., Van Stryland, E.W. (eds.), *Handbook of Optics* vol. 2 (2nd ed.), McGraw-Hill (1994) ISBN 0070479747.
24. Forward, R. L., "Grey Solar Sails," AIAA/ASME/SAE/ASEE 25th Joint Propulsion Conference, Monterey, California, July 10-14, 1989, AIAA Paper 89-2343.
25. Forward, R. L., "Grey Solar Sails," The Journal of the Astronautical Sciences, Vol. 38, No. 2, April-June 1990, pp. 161-185.
26. McInnes, C. R., *Solar Sailing – Technology, Dynamics and Mission Applications*, Springer-Verlag, 2004.
27. Norris, G., "Power Options," Aviation Week & Space Technology, October 4, 2010, pp. 48, 49, 51.
28. Union of Concerned Scientists, "Satellite Database." Online. Available **http://www.ucsusa.org/nuclear_weapons_and_global_security/space_weapons/technical_issues/ucs-satellite-database.html**, July 1, 2010.
29. Hudgins, E. L., ed., Space: The Free-Market Frontier, Cato Institute, 2002, p. 230.

30. Clark, J. S., George, J. A, Gefert, L. P., Doherty, M. P., and Sefcik, R. J., "Nuclear Electric Propulsion: A "Better, Safer, Cheaper" Transportation System for Human Exploration of Mars," NASA/TM 106406, Prepared for the 11th Symposium on Space Nuclear Power and Propulsion Systems sponsored by the University of New Mexico, Albuquerque, New Mexico, January 9-13, 1994.

31. NASA Mars Exploration Program, Online: http://mars.jpl.nasa.gov/programmissions/missions/.